Exploring fatty acid derivatives from renewable resources as raw materials for coating applications

Samer Nameer

Doctoral Thesis

KTH Royal Institute of Technology, Stockholm 2019
Fibre and Polymer Technology

Akademisk avhandling som med tillstånd av KTH i Stockholm framlägges till offentlig granskning för avläggande av teknisk doktorsexamen onsdag den 29:e Maj 2019, kl. 10:00 i sal F3, KTH, Lindstedtsvägen 26, Stockholm. Avhandlingen försvaras på engelska. Fakultetsopponent: Professor Dean Webster från North Dakota State University (USA)

TRITA-CBH-FOU-2019:28
ISSN 1654-1081
ISBN: 978-91-7873-184-8

To my family

Abstract

In the work presented herein, epoxy fatty acid derivatives were explored in the formation of thermosets for coating applications. The epoxy fatty acid derivatives were obtained from renewable resources such as birch tree bark and epoxidized linseed oil. The birch bark was used to isolate 9,10-epoxy-18-hydroxyoctadecanoic acid (EFA) and the epoxidized linseed oil was used to retrieve methyl stearate and 3 different epoxy methyl esters: epoxy methyl oleate/linoleate/linolenate (EMO/EMLO/EMLEN). The obtained epoxy fatty acid derivatives were used in resin formulations together with other reactants or in the synthesis of multifunctional oligomer resins using enzyme catalysis. All resins were cured using different polymerization techniques to form thermosets with a wide variety of properties.

Multifunctional oligomer resin were synthesized using *Candida Antarctica* lipase-B (CALB) as enzyme. It was demonstrated that the synthesis was efficient and the oligomers were obtained from “one-pot” route. In addition, the selectivity of CALB was useful in preserving a variety of functional groups (epoxides, alkenes and thiols) in the final oligomers. The oligomers were cross-linked by either thiol-ene chemistry or cationic polymerization resulting in functional thermosets. It was further shown that surface properties of the cured thermosets could be changed by using post-functionalization.

Pure fatty acid methyl esters cure into soft materials. An approach in increasing the thermal and mechanical properties was investigated. The 3 different epoxy functional methyl esters together with a furan-2,5-dicarboxylic acid derivative were investigated in the formation of thermosets. Glass transition temperature (T_g) below 0 °C and above 100 °C were obtained by varying the stoichiometric feed of the reactants.

The thermal curing of EFA as a one-component system was investigated by model studies showing that a self-catalyzed process occur. EFA thermally cures into a thermoset without the need of an added catalyst. Furthermore, the thermoset showed adhesive properties.

Crude mixture containing methyl stearate, EMO, EMLO and EMLEN obtained from epoxidized linseed oil were investigated as reactive diluent in coil-coatings. The mixture was also compared with commercially available reactive diluents such as fatty acid methyl esters (FAME) obtained from rapeseed oil. The results obtained showed that more fatty methyl esters could be incorporated in the final thermoset when using the epoxidized linseed oil fatty acid derivatives.

Real-time Fourier-transform infrared spectroscopy (RT-FTIR) was used during most of the work presented in the thesis and proved to be a powerful tool in monitoring the different reactions and comparing relative reaction rates.

Sammanfattning

I arbetet som presenteras i denna avhandling undersöktes epoxifettsyraderivat vid bildandet av härdplaster för ytmodifieringsapplikationer. Förnybara råvarorna björkbark och epoxiderad linolja andändes för att erhålla epoxifettsyraderivaten. Björkbarken användes för att isolera 9,10-epoxi-18-hydroxidekansyra (EFA) och epoxoderad linolja användes för att extrahera metylstearat och 3 olika epoximetylestrar: epoximetyl oleat/linoleat/linolenat (EMO/EMLO/EMLEN). Epoxifettsyraderivaten användes i olika hartsformuleringar tillammans med andra reaktanter eller vid syntes av multifunktionella oligomerhartser med hjälp av enzymatisk katalys. Med hjälp av olika polymerisationstekniker så härdades alla hartser till härdplaster med en mängd olika egenskaper.

Multifunktionella oligomerhartser syntetiserades med hjälp av enzymet *Candida Antarctica* lipas-b (CALB). Syntesen visade sig vara effektiv och oligomererna erhölls från en sats. Dessutom var selektiviteten hos CALB användbar för att bevara en mängd olika funktionella grupper (epoxider, alkener och tioler) i de slutliga oligomererna. Tiol-ene kemi eller katjonisk polymerisation användes sedan för att härda oligomererna, vilket resulterade i funktionella härdplaster. Vidare visades att ytegenskaperna kunde ändras genom möjlighet till funktionalisering av härdplasterna.

Mjuka material återfås då man härdar rena fettsyrametylestrar. Ett sätt att öka de termiska och mekaniska egenskaperna undersöktes. De tre olika epoxifunktionella metylestrarna tillsammans med furan-2,5-dicarboxylsyraderivat blandades i hartser och härdades. Genom att variera de stökiometriska förhållanderna av reaktanterna så erhölls glastemperaturer (T_g) under 0°C och över 100 °C.

Undersökningen av termisk härdning av EFA som ett komponentssystem studerades genom modelstudier. Studierna visade att en självkatalyserad process sker då EFA värms upp. Detta leder således till att EFA kan termiskt härda utan behov av en tillsatt katalysator. Dessutom uppvisade härdplasten limegenskaper.

Rå blandning innehållande metylstearate, EMO, EMLO och EMLEN som erhölls från epoxiderad linolja undersöktes som en reaktiv utspädare i spolbeläggningar. Blandningen jämfördes även med kommersiellt tillgängliga utspädare så som fettsyrametylestrar (FAME) erhållna från rapsolja. De erhållna resultaten påvisade att fler feta metylestrar kunde integreras i slutliga beläggningen när fettsyraderivat från epoxideradlinolja användes.

Realtids Fourier-transform infrarödspektroskopi (RT-FTIR) användes under det mesta av arbetet som presenteras i denna avhandling. RT-FTIR visade sig vara ett kraftfullt vektyg för att övervaka de olika reaktionerna samt jämföra relativa reaktionshastigheter.

List of papers

Paper I.

“One-component Thiol-Alkene Functional Oligoester Resins Utilizing Lipase Catalysis”, Finnveden, M.; **Nameer, S**.; Johansson, M.; Martinelle, M., Macromol. Chem. Phys. **2016**, 217, 1335-1341

Paper II.

“One-pot enzyme-catalyzed synthesis of dual-functional polyester macromers towards surface-active hydrophobic films”, **Nameer, S.**; Semlitsch, S.; Martinelle, M.; Johansson, M., J, RSC Adv., **2017**, 7, 50294

Paper III.

"Biobased Cationically Polymerizable Epoxy Thermosets from Furan and Fatty Acid Derivatives”, **Nameer, S.**; Larsen, D. B.; Duus, J.; Daugaard, A.; Johansson, M., ACS Sustainable Chem. Eng. **2018**, 6, 9442-9450

Paper IV.

“Fully bio-based aliphatic thermoset polyesters via self-catalyzed self-condensation of multifunctional epoxy monomers directly extracted from natural sources”, **Nameer, S.**; Johansson, M., J. Coat. Technol. Res., **2017**, 14, 757-765

Paper V.

“Bio-based multifunctional fatty acid methyl esters as reactive diluents in coil-coatings”, **Nameer, S.**; Deltin, T.; Sundell, P. E.; Johansson, M. *Manuscript*., **2019**.

Author contributions

My contribution to the appended papers:

Paper I.

Part of the experimental work, analysis and preparation of manuscript. Enzymatic synthesis and analysis of the oligomers was made by Maja Finnveden.

Paper II.

Most of experimental work, analysis and preparation of manuscript. Enzymatic synthesis of thiol-epoxy oligomer was made by Stefan Semlitsch.

Paper III.

Part of the experimental work, analysis and preparation of manuscript. Reactive DSC experiments and calculations from reactive DSC and relative reaction rates from RT-FTIR was made by Daniel Larsen.

Paper IV.

All the experimental work and analysis and most of manuscript preparation

Paper V.

Most of the experimental work, analysis and manuscript preparation. Simulated coil-coating experiments was made by Tomas Deltin at PTE Coatings AB, Hammarsv. 4, 594 31 Gamleby.

Abbreviations

^{13}C	Carbon-13
^{1}H	Hydrogen-1
ATR	Attenuated total reflection
BPO	Benzophenone
CALB	Immobilized Candida Antarctica lipase-B (Novozyme 435)
$CDCl_3$	Deuterated chloroform
Đ	Polydispersity index
DAFDC	Diallyl furan-2,5-dicarboxylate
DGEBA	Bisphenol A diglycidyl ether
DGFDC	Diglycidyl furan-2,5-dicarboxylate
DMTA	Dynamic mechanical thermal analysis
DSC	Differential scanning calorimetry
DP	Degree of polymerization
E’	Storage modulus
E”	Loss modulus
EFA	9,10-epoxy-18-hydroxyoctadecanoic acid
e-FAME	Mixture of methyl stearate, EMO, EMLO and EMLEN
ELO	Epoxidized linseed oil
EMLEN	Epoxy methyl linolenate
EMLO	Epoxy methyl linoleate
EMO	Epoxy methyl oleate
EtOAc	Ethyl acetate
FDCA	2,5-furandicarboxylic acid
FTIR	Fourier-transform infrared spectroscopy
FT-Raman	Fourier-transform raman spectroscopy
G’	Shear modulus
H_2O	Water
H_2SO_4	Sulphuric acid
HFA	Heneicosafluorododecyl acrylate
HMVE	1,6-hexanediol mono vinyl ether
LA	Lauryl acid
LOH	Lauryl alcohol
MALDI	Matrix-assisted laser desorption/ionization
MCh	6-mercapto-1-hexanol
MeOH	Methanol
$MgSO_4$	Magnesium sulphate
M_n	Number average molecular weight
MUD	11-mercaptoundecanol

M_w	Weight average molecular weight
NaOH	Sodium hydroxide
NMR	Nuclear magnetic resonance spectroscopy
RT-FTIR	Real-time Fourier-transform infrared spectroscopy
SH-Ene	Thiol-alkene telechelic resin
SH-Epoxy	Thiol-epoxy telechelic resin
T_g	Glass transition temperature
Tan δ	Tan delta
UV	Ultraviolet

Table of contents

1. Introduction

1.1 The sustainable development goals adopted by the United Nations

During the year of 2015 the governmental leaders of the world agreed upon 17 sustainable development goals (SDGs) aiming for a better planet by the year 2030.[1] The goals raise both humanitarian and ecological issues that need to be addressed. Regarding the ecological issues, many of these goals relate to a sustainable future hence, framework consisting of actions have been adopted in order to guide the society in a sustainable pathway.

Many of the SDGs are closely related for example one of the actions discussed in Goal 9: Industry, Innovation and Infrastructure, is the need for technological advances in order to achieve environmental objectives enabling sustainable industrialization. One way to meet this action is to promote scientific research utilizing natural resources. Goal 9 is closely linked to Goal 12: Responsible Consumption and Production and Goal 13: Climate Action, which further acknowledge the utilization of environmentally benign resources.

In addition, the life in water and on land are discussed in respectively, Goal 14: Life below Water and Goal 15: Life on Land. The targets discussed relate to protect life in our oceans and our forests by not harming the biodiversity. One example of an issue are the plastic waste our oceans and non-degradable waste in landfills. One example of meeting these actions is to promote scientific research regarding biodegradable materials. In addition, there is a need to develop better processes and protocols on how the society should manage waste in a better way.

The work behind this thesis relates to discussed SDGs by the utilization of renewable resources that are considered environmentally benign. Furthermore, on how building-blocks can be obtained from the renewable resources and subsequently applied in different coating applications.

1.2 Purpose of the study

With the environmental awareness and the adopted SDGs by the United Nations in mind, there is a growing interest in utilizing environmentally benign resources as alternative to fossil-based. One example of resources that are considered as environmentally benign are renewable resources. In the context of polymer chemistry different renewable resources are explored as alternatives in the pursuit of finding new bio-based monomers. In addition, technical challenges lies in utilizing the obtained monomers through benign procedures in order to adopt sustainable protocols. Moreover, other challenges such as properties of the final material in an application needs to be met.

The main purpose of the study for this thesis work relies in the aspect of utilizing renewable resources in the extraction of epoxy based monomers that subsequently can be used in different coating applications. The more specific purposes was using sustainable practices as much as possible and understanding of structure-property relationships of the formed thermosets. In addition, the gained structure-property knowledge could then be used to target specific material properties.

Following goals were aimed during the work for this thesis:

1. Isolation of epoxy fatty acid derivatives from renewable resources such as birch tree bark and epoxidized linseed oil and use them in the formation of thermosets for different coating applications
2. Using enzymatic catalysis as a benign synthetic route in the formation of multifunctional resins from the obtained epoxy derivatives. In addition, obtain thermosets with surface post-modification opportunities.
3. The ability to tune the final thermal and mechanical properties of thermosets obtained from the epoxy based fatty acid derivatives with a furan-2,5-dicarboxylic acid derivative.
4. To obtain clear-coats that have possible commercial application in coil-coatings containing the epoxy fatty acid derivatives.

2. Background

2.1 Renewable resources as raw material for polymer synthesis

Polymer materials are an integral part of our modern society and can be found in a vast amount of applications in our daily life.[2] One of the largest polymer material groups are synthetic polymers such as thermoplastics and thermosets derived from fossil-based resources. Their production has increased dramatically from 2 Mt per year in 1950 to >300 Mt per year in recent years.[3] The market success of polymer materials has enabled the high standard of living that has evolved during the 20th century. Some examples of their success can be found in applications enabling lighter cars,[4] longer food preservation[5] and effective drainage systems.[6] However, concerns have been raised lately regarding the durability and end-life of synthetic polymers.[7,8] Due to both depleting fossil resources[9] and the negative impact that plastics continue to have on the environment,[10] alternative resources are being explored as replacements to the current fossil-based. Renewable resources are considered as a promising replacement to fossil-based materials, in order to address these challenges.[10] However, the use of renewable resources have to increase significantly in both volume and number of applications to meet the market demands and fulfil a future sustainable society.[11–13] The utilization of renewable resources is not a new approach.[10] Abundant building-blocks from nature have previously been used in the making of novel polymeric materials such as alkyds,[14,15] cellulose acetate,[16] vulcanized natural rubber,[17] to mention but a few. Building-blocks from renewable resources such as forests and annual crops and plants are considered as favorable environmental alternatives due to their availability and reduced greenhouse gas emissions.[18–20] In addition, from a chemical point of view, the wide molecular diversity provided from renewable feedstock (e.g. cellulose, lignin, hemicellulose, fatty acids, sugars and proteins) are beneficial for the production of novel functional polymer materials.[10,21]

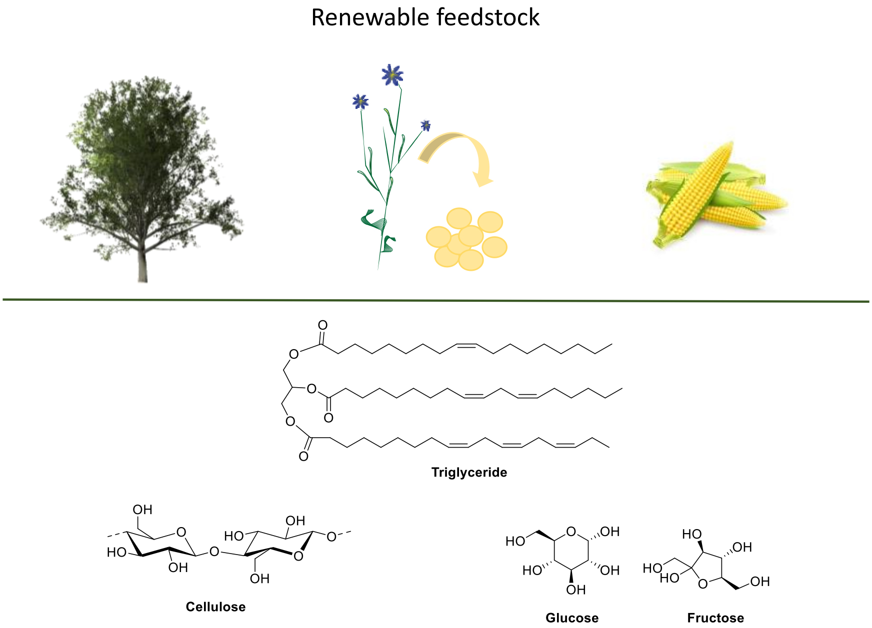

Figure 1: Examples of renewable resources and some examples of building-blocks that can be obtained from them. Corn cobs in the figure was designed by macrovector / Freepik

2.2 Fatty acid derivatives from renewable resources

One specific group of renewable compounds that have been used for a long time in material applications is fatty acid derivatives, which have been used as drying oils in paints[22] and in alkyds[14]. The highly reduced state and diversity of functional groups available, make fatty acids very suitable as raw materials. A wide variety of fatty acids exist and can be found in different abundant natural systems including tree bark, plants and crops.[10] The following paragraphs will discuss the different resources used in this thesis work containing fatty acid derivatives.

2.2.1 Outer birch tree bark and plants as renewable resources

The external tissue layer of plants is formed as a protective barrier containing wax and a natural aromatic-aliphatic polyester network called suberin or cutin.[10,23,24] The role of suberin and cutin in plants includes control of water loss and protection against pathogens.[10] Suberin is found in bark of birch tree (*Betula Pendula)* or cork oak (*Quercus suber*) or in potato peel while cutin is found in leaves, fruits and stems.[10,23] The macromolecular structure of both suberin and cutin is complex and has not been fully determined, although schematic structures of the macromolecular network has been proposed in literature.[23–26] Pioneering work from Kolattukudy[27] and Holloway[28] have characterized the main building-blocks being ω-hydroxyl fatty acids, α,ω-dicarboxylic acids and phenolic compounds (Figure 2). Lately glycerol has also been added as a component.[29] In addition, physically bound building-blocks have been characterized to be triterpenoids.[30,31] The fatty acid monomers can be extracted by breaking the ester linkages through depolymerization of the macromolecular structure using alkaline hydrolysis[32] or methanolysis.[29] Subsequently, isolation methods are performed to obtain the building-blocks of interest.[32] The mentioned α,ω-fatty acids have yet not been found abundant in other resources in nature, thus making both suberin and cutin interesting as a renewable source for the extraction of these compounds.[10]

Large amounts of suberin can be found in the outer birch tree bark (*Betula Pendula*)[33,34] and cork oak tree bark (*Quercus suber L*).[29,34] Previous studies have shown that outer birch tree bark contain approximately 10 % of the monomer 9,10-epoxy-18-hydroxyoctadecanoic acid (EFA).[34] A relatively new report published in 2014 from Innventia (now RISE), a research institute in Sweden, showed that the pulp and paper industry of Sweden and Finland together produces 255 000 tons annually of birch tree bark as a by-product.[35] The exact amount of suberin has not yet been determined, however, it is estimated to be 20-50% of the bark.[36] This suggests that between 51 000 – 127 500 tons of suberin building-blocks could potentially be retrieved. Traditionally the bark is incinerated for energy recovery, thus considered as a low value side stream.[35,37] Instead of burning the bark, inherent building-blocks from the suberin structure could be extracted and utilized in the chemical industry for different purposes, thereby creating added value to the biomass side-stream.

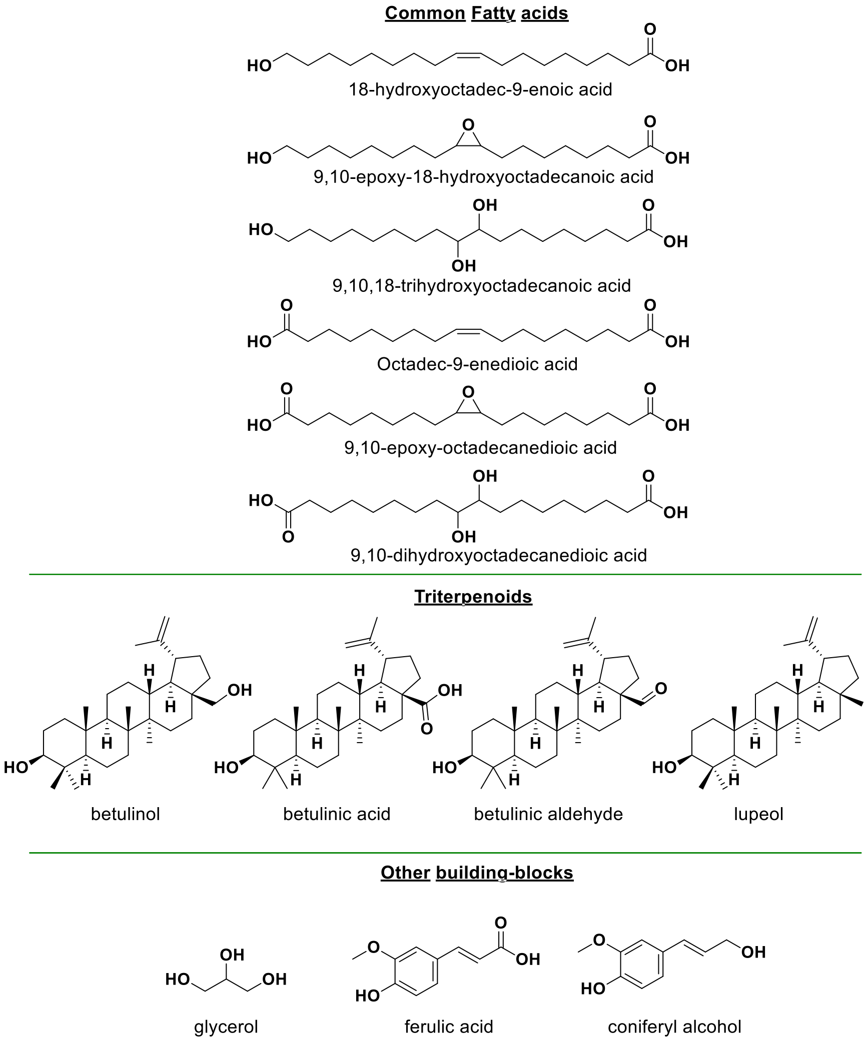

Figure 2: Common compounds found in outer birch tree bark suberin previously reported.[30,36]

2.2.2 Vegetable oils from renewable resources

Another renewable raw material that shows promise due to its low cost and availability, are vegetable oils.[18,20,38] Vegetable oils can be found in annual crops such as flax, linseed, soybean, sunflower and rapeseed.[18,38,39] The production of vegetable oils has steadily been increasing in recent years and amounted to >180 Mt in 2017/2018.[40] They are produced in a large scale thus making them feasible as a renewable feedstock in the polymer industry.[18,38] The oils are mainly composed from triglycerides i.e. a glycerol unit connected by ester bonds with three fatty acids (Figure 3).[18] The fatty acid composition varies and depends on the crops, environment and season.[41] Common fatty acids found in vegetable oils include C14, C16 and C18 in different variations of unsaturations and other functional groups.[18–20,38] Table 1 shows some commonly used vegetable oils and their respective composition of C18 fatty acid chain. The use of vegetable oils dates back centuries:[42,22] they have been utilized in many different coating applications as air-drying oils or incorporated in alkyd resins.[14,43–45] The air-drying ability of the vegetable oils lies in the reaction of the unsaturations with oxygen in air.[46] One example of a vegetable oil that undergoes auto-oxidation is linseed oil where the high amount of unsaturations within the fatty acid chains results in air-drying properties used in coating applications such as paints, varnishes and lacquers.[46,47] Although linseed oil had been used for centuries in coating applications, during the adoption of fossil-based molecules there was a limited use of fatty acids.[48] With the increasing interest on utilizing renewable resources, vegetable oils and their fatty acid derivatives are becoming more compelling for use the chemical industry.[10,18,20,38] Lately novel resins with a wide range of applications as thermosets have been synthesized from fatty acid derivatives such as sucrose based epoxidized fatty acids,[49] acrylate based fatty acid derivatives,[50] and multi-functional epoxy fatty acid resins.[51]

In order to obtain free fatty acid derivatives, the ester bond between the glycerol unit and the connected fatty acids need to be cleaved. This has previously been reported utilizing alkaline methanolysis[52] or biocatalysis[53].

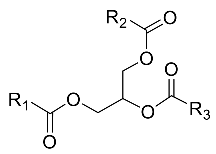

Figure 3: General chemical structure of triglyceride.[18] The different R-groups can be found in Table 1.

Table 1: Common vegetable oil types and their respective composition.[54] X indicate carbon chain length and Y indicate number of unsaturation. For this thesis work, only C18 fatty acid chains were considered.

R(x:y)	18:0	18:1	18:2	18:3
Linseed oil	4	22	15	52
Soybean oil	5	21	53	8
Rapeseed oil	1	60	20	9

2.2.2.1 Epoxidized fatty acid derivatives

Epoxidized fatty acid derivatives can be found in some natural sources. As earlier mentioned they can be found in suberin and cutin.[10,23] In addition, vernolic acid, an epoxy fatty acid, can also be found in oil seed crops such as *Euphorbia lagascae* or *Vernonia galamensis*.[52,55] Epoxidation of the unsaturations on vegetable oils can be obtained from a performic acid reaction[56] or from benign synthesis routes utilizing biocatalysis.[57–59] Due to the high ring-strain, epoxides provide a versatile platform in the formation of many different polymeric materials. Epoxides have previously been applied in the formation of polycarbonates,[60,61] epoxy-anhydride thermosets[49,62] and epoxy-amine systems.[63,64]

2.3 Benign synthesis methods

Enzymes are naturally existing three-dimensional catalytic proteins built up from amino acids. The role of enzymes in nature is to participate in different reactions as catalysts; including hydrolysis, oxidation, and reduction reactions.[65,66] One of the most beneficial advantages of enzymes are their high selectivity towards a specific substrate. The high selectivity originates from the active site which is a defined cavity within the three-dimensional structure of the enzyme.[67] The selective property lies in the aspect of the "key-lock" mechanism, theorized by Fischer in 1894,[68] where the substrate perfectly fits in the active site like a "key in a lock". Hence, the active site decides what kind of reaction the enzyme is intended to catalyze. For example the hydrolases (type of enzymes) participate in hydrolysis cleavage of a specific substrate.[69] A general illustration of the reaction pathway can be seen in Figure 4, which compares catalyzed with uncatalyzed processes.[66] Due to the enzyme-substrate interaction a lower energy pathway to the product can be obtained in comparison to the uncatalyzed procedure. Other than being highly selective, enzymes are considered environmentally benign, efficient and can operate under mild condition.[66,67,70] From a chemist point of view there are also some drawbacks to utilizing enzymes, such as narrow operation parameters, some loss of catalytic activity in organic solvents and substrate or product reaction inhibition.[66]

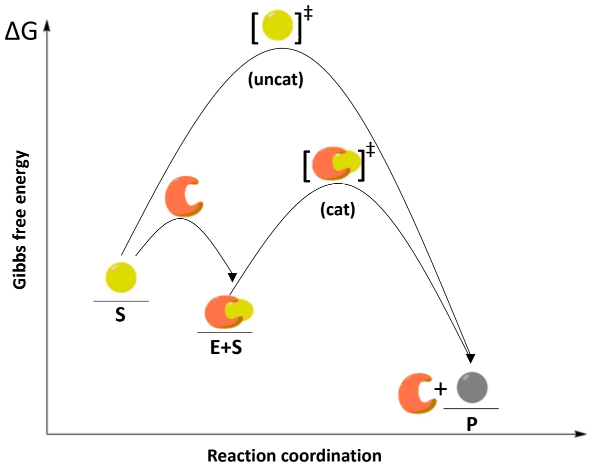

Figure 4: General schematic of the energy pathways of an enzyme catalyzed and uncatalyzed reaction.

2.3.1 Lipase catalysis in polymer chemistry

Polyesters are a group of polymers that are interesting within polymer science, as they are used in a large number of applications and can be found in, for example, fibers, textiles and packaging.[71] One very successful polyester is poly(ethylene terephthalate) (PET) which is widely used as packaging for carbonated drinks.[2] Polyesters are polymers containing ester functional groups in their back bones.[71] The formation of ester bonds can occur from the reaction of diols with diacids, which results in the elimination of water.[71] Traditional polymer synthesis of polyesters require high temperatures and catalysts.[17,72] In addition, in order to preserve substrate functional-groups of interest, protection and deprotection step procedures are often employed.[73–75] In the pursuit of benign synthesis routes, enzyme catalysis has been utilized in polymer chemistry.[76, 77] Lipases are a group of enzymes that has attracted extensive interest as catalysts due to their versatility.[78,79] In addition, they can operate under mild conditions in organic solvents or in bulk.[78] In biological systems lipases are responsible for the hydrolysis reaction of triglycerides i.e. cleaving the ester bond between glycerol and fatty acids.[69,76,80] Considering that enzymatic reactions are in chemical equilibria, one can reverse the hydrolysis reaction and form ester bonds through condensation reactions. One specific lipase that has gained significant interest in polymer science is *Candida Antarctica* lipase-B (CALB).[78] The catalytic activity in CALB emerges from the amino acid triad, Ser105-His224-Asp187.[81] As an example, a transesterification reaction catalyzed by CALB can be explained by Ser105 acting as a nucleophile on the substrate (e.g. ester) forming an enzyme-substrate complex also known as an acyl-enzyme complex.[78,82] A catalytic event occurs and alcohol leaves the active site. Consecutively a nucleophile (e.g. alcohol), also known as an acyl-acceptor, enters the active site and attacks the acyl-enzyme complex forming the final product (new ester).[78,82]

One example of immobilization of CALB on a microporous carrier, also known as Novozyme 435, has provided effortless lab procedures.[78] For example, the end of a reaction can be controlled by filtering the microporous carrier from the reaction mixture.[66,78] Furthermore, CALB has high selectivity towards hydroxyl groups over other functional groups.[83] This feature has been used in the formation of multifunctional polyesters, preserving functional groups of interest such as alkenes or epoxides.[84,85]

2.4 Polymer thermosets

Thermosets are one group of materials used for a wide range of applications such as adhesives, polymer composites, surface protection and/or esthetics, to mention a few.[86] The thermal and mechanical properties of the thermoset determine the final application.[87] In turn, the thermal and mechanical properties such as glass transition temperature (T_g) and stiffness depend on the chemical structures of the reactants, stoichiometric feed ratios and type of reaction involved, thus, knowing the intended application for a thermoset one can tailor the properties.[87] This implies that structure-property evaluation is essential in order to tailor a thermoset for the intended application.

Numerous different reactions may result in thermoset formation, such as two-component (2K) systems,[64] oxidative cross-linking,[46] thiol-ene coupling[88] and cationic polymerization.[89] However, in order to obtain cross-links, the starting monomers, oligomers or polymers should have a functionality of 2 or more.[87]

The work for this thesis has mainly focused on epoxy based thermosets from renewable resources. The epoxy functional group has a central role in thermoset formation due to the high reactivity of the epoxide towards numerous functional groups enabling a variety of chemical reactions in both basic and acidic conditions.[90,91] Epoxides have been applied in both photo-initiated[84] and thermally induced[63] curing of resins.

2.4.1 Photo-initiated curing

Photo-initiated polymerization can be utilized in order to readily form thermosets.[92–94] The technique finds applications within printing inks,[95,96] protective coatings,[97,98] dental restoration[99,100] and adhesives.[101] The main advantages of UV-curing includes rapid curing at ambient temperature and the absence of solvents.[88,93] During a typical procedure the intense UV-light yields a reactive species that initiates polymerization. Other process characteristics include solvent-free formulations and room temperature polymerization conditions.[92,94] One of the most studied groups for cationic polymerization is the epoxide group.

2.4.1.1 Cationic polymerization

Pioneering work from Crivello and Lam laid the ground for UV-initiated cationic polymerization in the discovery of diaryliodonium and sulfonium salts as latent sources for strong protonic acids.[102,103] One of the main advantages of using cationic polymerization is the absence of oxygen inhibition thus distinguishing the process from radical mediated photo-polymerization.[94,104] In addition, low shrinkage of the final thermoset is obtained.[94] Cationic polymerizations also display post-curing i.e. "dark-curing", where the initiated reaction continues after the UV-light has been turned off until all reactive species have been consumed.[94,103,104] Upon intense UV-light, the initiator dissociates and a strong protonic acid is formed, usually $HSbF_6$ or HPF_6.[102,103] Subsequently the strong acid protonates an epoxide monomer enabling chain-growth propagation (Scheme 1).[94,105] One of the main features required for the reaction to proceed is the non-nucleophilic character of the anion. The less nucleophilic character, the faster the reaction rate.[103]

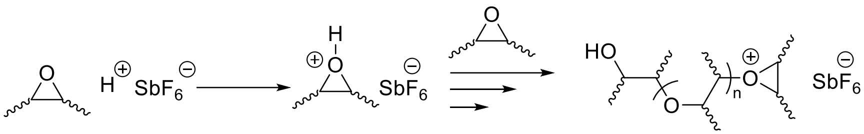

Scheme 1: General photo-initiated cationic polymerization.[105] Scheme shows only the protonation and chain-growth parts of the mechanism.

2.4.1.2 Thiol-ene chemistry

Another chemistry that has received attention in recent decades is polymerization using thiol-ene chemistry.[88,93] Advantages of thiol-ene chemistry include late gelation resulting in homogenous networks,[106] the occurrence of polymerization without a photo-initiator,[107] reduced effect of oxygen inhibition[108] and low shrinkage of the final network.[100] As the name refers, the reaction takes place between a thiol and alkene functional group following a free radical/step growth process. Scheme 2 shows a general reaction procedure. The reaction is established via photolysis of an initiator (PI) resulting in a generated radical species. Subsequently a hydrogen is abstracted from the thiol group by a radical species producing a thiyl radical. As a consequence the thiyl radical adds to an alkene forming a carbon centered radical. A new thiol species is then available for hydrogen abstraction regenerating the thiyl radical and the process continues in such fashion.[88,93,109] In an ideal thiol-ene reaction no homo-polymerization of the alkene occurs.[88] In contrast to conventional free radical reactions, the thiol-ene reaction is less effected by oxygen inhibition during the reaction procedure.[110] In free radical reactions of e.g. acrylates, oxygen acts as a scavenger of the radicals, resulting in termination of the reaction. In the case of thiol-ene the oxygen adds to a growing chain and forms a peroxy radical which in turn can abstract a thiol-hydrogen generating a thiyl radical that can participate in the propagation step and so on.[108]

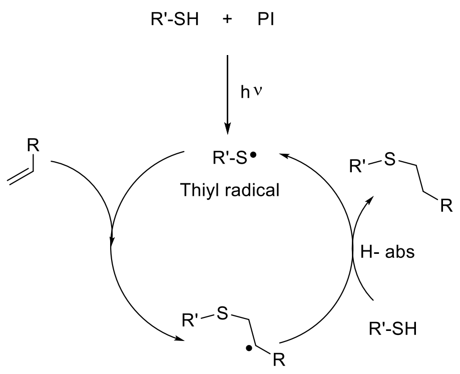

Scheme 2: General mechanism proposed for the thiol-ene reaction.[88]

2.4.2 Thermally induced curing

A common industrial practice is to utilize thermal curing for the formation of coatings. One example of this is the coil-coating process where sheet metals are pre-coated with a resin formulation.[47,111] The process is fast and continuous, thus high temperature convection ovens often reaching peak metal temperature (PMT) of 230-240 °C in order to cure the resin formulation.[47,111,112] Traditional resin formulations use solvents to obtain desirable rheological application properties.[47] Upon curing the solvents evaporate generating environmentally harmful volatile organic components (VOCs) that are incinerated for energy pruposes.[47,113,114] One way to overcome this is to add a reactive diluent which acts as a solvent and reacts into the final coating upon curing. In the context of utilizing renewable resources, fatty acid methyl esters (FAMEs) from rapeseed oil have previously been demonstrated as good reactive diluents.[115] During thermally induced curing many different reactions take place parallel to each other including condensation reaction, transesterification, etherification, oxidative cross-linking and ring-opening (if present). The FAME will thus initially act as a solvent and during the curing either evaporate or react and become an integrated part of the dry film.[112]

3. Experimental

The following experimental section briefly describes the experimental details. In order to obtain a more detailed description please see the appended papers (Papers I-V).

3.1 Abbreviation highlight

To simplify the discussion part of this thesis (Section 4) some of the materials used have been assigned abbreviations (Figure 5). For instance, 9,10-epoxy-18-hydroxyoctadecanoic acid is referred to as "EFA". The epoxidized fatty methyl esters; epoxy methyl oleate, epoxy methyl linoleate and epoxy methyl linolenate are referred to as "EMO", "EMLO" and "EMLEN" respectively. As a group EMO, EMLO and EMLEN are referred to as "EMX". The mixture of methyl stearate, EMO, EMLO and EMLEN is referred to as "e-FAME".

The furan-2,5-dicarboxylic acid is referred to as "FDCA". The di-allylated version of FDCA is called diallyl furan-2,5-dicarboxylate and is referred to as "DAFDC" while the di-glycidyl version of FDCA is called diglycidyl furan-2,5-dicarboxylate and is referred to as "DGFDC".

FAMEX or e-FAMEX are referred to as the amount in wt% of FAME or e-FAME used in the formulation, were X being 5, 10, 15 or 20 wt% of the whole coil-coating formulation.

The monomers lauryl alcohol and corresponding acid are referred to as "LOH" and "LA".

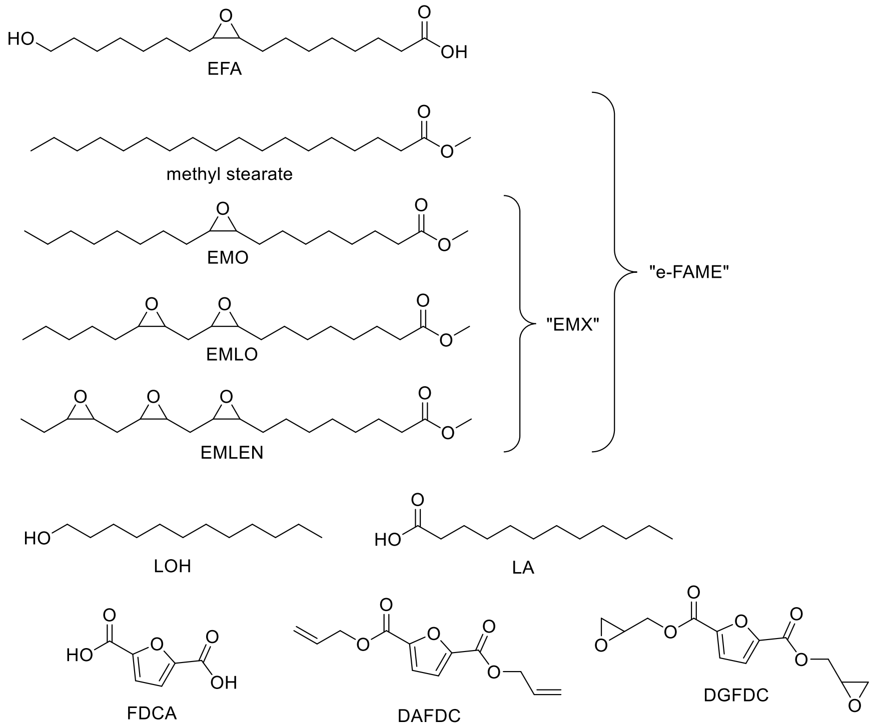

Figure 5: Highlighted chemical structures of used compounds in the work for this thesis.

3.2 Materials

The fatty acid derivatives were retrieved from natural resources. Outer birch tree bark (*Betula pendula*) was kindly supplied by Holmen AB and used for the retrieval of 9,10-epoxy-18-hydroxyoctadecanoic acid (EFA). Epoxidized linseed oil was kindly supplied by Acros chemicals and PTE Coatings AB and used for the retrieval of epoxidized fatty acid methyl esters; methyl stearate, epoxy methyl oleate (EMO), epoxy methyl linoleate (EMLO) and epoxy methyl linolenate (EMLEN). Rapeseed methyl esters (FAMEs) and two model coil-coating polyester/melamine (hexahydroxymethyl melamine (HMMM)) were kindly supplied by PTE Coatings AB. One of the coil-coating formulation containing 10wt% FAME and the second did not contain FAME. The polyester in the coil-coating formulations was hydroxyl functional with a hydroxyl value of 120.9 mg KOH/ g resin, acid value of 8 mg KOH/g resin and molecular weight (M_w) of 4000±500 g/mol. Hot dip galvanized steel substrates were kindly provided by SSAB EMEA. All materials were used as received.

3-Chloroperbenzoic acid (≤77%), 5,5'-dithiobis-(2-nitrobenzoic acid) (≥98%, Bioreagent), 6-mercapto-1-hexanol, 11-mercaptoundecanol (98%), bisohenol-A-diglycidyl ether, chloroform, cis-2-butene-1,4-diol (97%), dimethyl adipate (≥99%), dimethyl succinate (98%), ethyl acetate, sodium hydroxide (NaOH, reagent grade pellets, ≥98), sulfuric acid (H_2SO_4 (95-97%)), n-heptane, lauryl acid (natural, ≥98%, FCC, FG), lauryl alcohol, methanol, $MgSO_4$ (s), Novozyme 435 (immobilized *Candida Antarctica* lipase-B), phosphate buffer pH 7.0 (1M, 20 °C) were all supplied by Sigma-Aldrich and used as received.

Diallyl furan-2,5-dicarboxylate (DAFDC) was kindly supplied by Daniel Larsen from Danish Technical University when he was a visiting researcher in our group. The synthesis of DAFDC can be found in the literature.[116]

1,6-Hexanediol mono vinyl ether and the photo-initiator 2,2-dimethoxy-2-phenylacetophenone (Irgacure 651) were supplied by BASF. The photo-initiators p-(octyloxyphenyl)phenyliodonium hexafluoroantimonate (UVAcure 1600) and benzophenone (≥99%) were supplied by CYTEC and Fluka respectively.

3.3 Instrumentation

Nuclear magnetic resonance (NMR) was performed on a Bruker AM NMR. ^{1}H-NMR and ^{13}C-NMR spectra were recorded at 400 MHz and 101 MHz respectively. ^{1}H-NMR spectra were acquired using a spectral window of 20 ppm, a relaxation delay of 1 second and 16 scans. ^{13}C-NMR spectra were acquired using a spectral window of 240 ppm, a relaxation delay of 2 seconds and 512 scans unless otherwise stated. Analyses of obtained spectra were performed using MestReNova version 9.0.0 - 12821 (Mestrelab Research S.L 2013).

Fourier-Transform Infrared Spectroscopy (FTIR) and *in situ* real-time FTIR (RT-FTIR) analyses were performed on a PerkinElmer Spectrum 2000 FTIR or PerkinElmer Spectrum 100 both equipped with a heat controlled single reflection attenuated total reflection (ATR) accessory (Golden Gate heat controlled) from Graseby Specac Ltd (Kent, England). For

FTIR, the spectra were collected by recording data based on 8-16 scans with a resolution of 4 cm^{-1} and a range of 600 to 4000 cm^{-1}. For *in situ* RT-FTIR, analysis was carried out continuously at a rate of 1 scan per 5.2 seconds with a 4 cm^{-1} resolution (Figure 6). A quartz glass cover slide were used for photo-initiated experiments. The data from FTIR and RT-FTIR were processed and analyzed in Spectrum software v. 10.5.1 and TimeBase® respectively. Samples for RT-FTIR analysis are detailed under section 3.4.2. In order to monitor the polymerization performance and chemical structure during network formation characteristic absorbance peaks of interest were evaluated (Table 2).

Table 2: FTIR characteristic absorbance peaks of interest for this thesis work

Chemical structure	Characteristic absorbance on FTIR[a]
Hydroxyl (R-OH)	3500 – 3300 cm^{-1} (O-H, ν_{str})
Alkene ($RCH=CH_2$)	1680 – 1620 cm^{-1} (C=C, ν_{str})
Aliphatic ether (R-O-R')	1150 – 1060 cm^{-1} (C-O-C, ν_{asym})
Carboxylic acid (R-C(O)-OH)	1715 – 1700 cm^{-1} (C=O, ν_{str})
Ester (R-C(O)-O-R)	1750 – 1715 cm^{-1} (C=O, ν_{str})
Epoxide ring (-C-O-C- , ring)	950 – 750 cm^{-1} (-C-O-C- ring, ν_{asym})

[a] Reference[117]

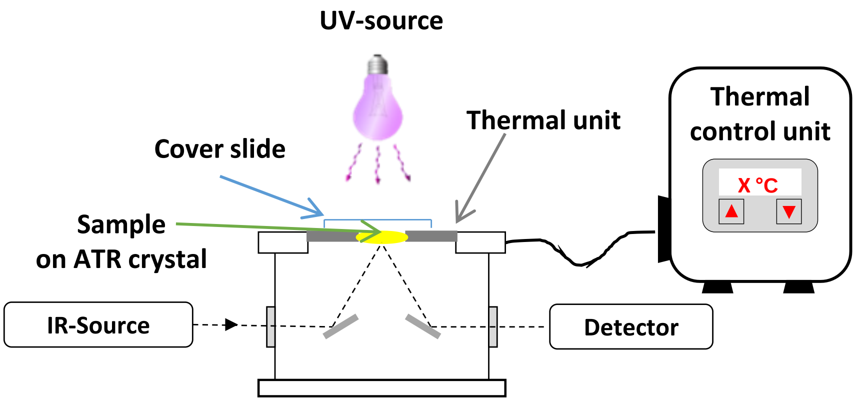

Figure 6: Overview of the RT-FTIR setup.

Fourier-Transform Raman Spectroscopy (FT-Raman) analyses were performed on a PerkinElmer Spectrum 2000 NIR FT-Raman instrument equipped with a Nd-YAG laser. The spectral data were based on 32-64 scans recorded with a laser power of 500-1000 mW. The performance of the polymerization and the assessment of the chemical structure during network formation were based on the evaluation of the alkene and thiol absorbance peaks (Table 3).

Table 3: FT-Raman characteristic absorbance peaks of interest for this thesis work.

Chemical structure	Characteristic absorbance on FT-Raman[a]
Alkene ($RCH=CH_2$)	1680 – 1620 cm^{-1} (C=C, ν_{str})
Thiol (-S-H)	2600 – 2540 cm^{-1} (S-H, ν_{str})

[a] Reference[117]

Automated column chromatography was carried out using an Isolera 4 advanced automated flash purification system from Biotage, LLC (Charlotte, NC, USA) equipped with a UV detector. Prepacked 50 g silica Biotage KP-Sil columns were used as the stationary phase. A gradient of n-heptane/EtOAc was used as the mobile phase to separate the mixture. The prepacked columns were loaded with approximately 10wt% of sample relative to the column silica weight.

Matrix-assisted laser desorption/ionization time of flight mass spectroscopy (MALDI-TOF-MS) was performed on a Bruker UltraFlex MALDI-TOF MS equipped with SCOUT-MTP Ion Source (Bruker Daltonics, Bremen), gridless ion source, a N_2-laser operating at 337 nm and a reflector design. SpheriCal™ calibrants were used to calibrate the system and the detector was set to 200-2500 *m*/*z*. The spectra were collected using a reflector-positive method. The accelerating voltage was set to 25 kV and the reflector voltage was set to 26.3 kV. A solution containing tetrahydrofuran (THF) and 2,5-dihydroxybenzoic acid (DHB) was used as a matrix and sodium trifluoroacetate (NaTFA) was used as a counter-ion. The collected spectral data were analyzed with FlexAnalysis version 2.2 from Bruker Daltonics.

The UV-light source Hamamatsu L5662 was used for the UV initiated experiments. The instrument was equipped with a standard medium-pressure 200 W L6722-01 Hg-Xe lamp. In order to measure the intensity a

Hamamatsu UV-light power meter (model C6080-3) calibrated for 365 nm main emission line was used. The intensity of the lamp was measured before and after the experiments and was stable at approximately 50 mW cm^{-2}.

Differential scanning calorimetry (DSC) was conducted on a Mettler Toledo DSC-1 equipped with Gas Controller GC100. Approximately 5-10 mg of sample was weighed for analysis. The aluminum crucibles used for both references and samples were 100 µL. An inert nitrogen atmosphere was used for all systems.

The DSC were used for 2 purposes. Purpose 1 was to obtain the T_g of formed thermosets. This was made on thermosets from telechelic resins, EMX-DGFDC and e-FAME coil-coatings. Purpose 2 was to obtain reactive thermograms from the EMX-DGFDC system.

Purpose 1: when the DSC was used in order to obtain T_g the data collection was based on heating/cooling cycles with 5 min isotherms in-between. The T_g was reported from the midpoint of the second heating cycle. Table 4 shows the different parameters for the analysis and respective thermoset sample analyzed.

Table 4: The table shows the different samples and their respective parameters during DSC analysis in order to obtain T_g values.

Thermoset sample from	Temperature (°C)	Temperature rate (°C min^{-1})
Telechelic resins	-60 to 150	5
EMX-DGFDC system	-50 to 200	10
e-FAME coil-coatings	-50 to 200	10

Purpose 2: When the DSC was used in order to obtain reactive DSC of the EMX-DGFDC system, the reactants were mixed in 1:1 epoxy molar ratio and UVAcure 1600 was added amounting to 2wt% of the total monomer weight. The data collection was based on heating/cooling cycles with 5 min isotherms in-between. The temperature range was set to 25 to 300°C with temperature rate of 10 °C min^{-1}.

Dynamical mechanical thermal analysis (DMTA) was performed on a Q800 DMTA (TA Instruments) equipped with a clamp for tensile testing. The data were collected relative to a temperature ramp from -50°C to 200°C with a heating rate of 3 °C min^{-1}. The oscillating amplitude was set to 0.1% of the sample length given from the DMA instrument. Preload was set to 0.010 N, frequency to 1 Hz and force track to 125%. The T_g was obtained from the tan δ peak. The dimensions of the samples were 4-5 mm in width, 20-30 mm in length and 0.2-0.3 mm in thickness. Cross-link densities were calculated from Eq. 1

$$E' = 3\nu_e RT \qquad \text{Eq. (1)}$$

Where, E' is the storage modulus in the rubbery plateau, ν_e is the cross-link density, R is the gas constant and T is the absolute temperature.

Rheological measurements were conducted on a TA Instruments (New Castle, DE, USA) Discovery Hybrid 2 (DHR2) rheometer equipped with a Peltier plate containing temperature control. A parallel-plate geometry of 25 mm was used during viscosity measurements and 8 mm for evaluation of shear modulus (G'). For the viscosity measurements the sample (0.5 – 1 mL) was pipetted onto the Peltier plate heated to 30 °C. The parallel plate was lowered to a gap height of 0.5 mm. Samples exceeding parallel-plate size were trimmed using a straight spatula. The viscosity experiments were evaluated on flow sweep mode of scouting mission of torque 0 – 1000 µNm. The steady state constant viscosity was reported from the evaluations. For the G' measurements the sample was put on the peltier plate. Stress sweep followed by frequency sweep were both assessed in the linear viscoelastic region. Temperature sweep was evaluated from -25 °C to 40 °C with temperature rate of 5 °C min^{-1}. The stress was set to 2000 Pa and a constant angular frequency of 10 rad s^{-1}. All rheometry data were processed in TRIOS a TA Instrument software.

Contact angle measurements were based on static contact angle measurements. The analysis was carried out on a CAM 200 contact-angle meter (KSV Instruments, Helsinki, Finland). The instrument was equipped with a Basler A602f camera. For the measurement the sessile-drop technique was used and an approximately 3 µL MilliQ water droplet was dispensed on the surface by an automatic dispenser. Five different spots of the sample surface were recorded. Contact angles using Young-Laplace fittings were assessed by OneAttention software.

3.4 Synthetic procedures

3.4.1 Retrieval of fatty acid derivatives from renewable resources

Two different renewable resources were evaluated in order to obtain fatty acid derivatives.

3.4.1.1 Retrieval of 9,10-epoxy-18-hydroxyoctadecanoic acid (EFA) from outer birch bark

The retrieval of the fatty acid EFA from outer birch bark (*betula pendula*) has previously been reported.[32] The extraction procedures were followed with minor modifications. In order to retrieve EFA from the bark, first the outer birch bark needed to be grinded into powder. Extractives from the powder were then removed by utilizing soxhlet extraction in n-heptane 3 times for 8 hours each time. After this, the wet powder was left to dry in a fume hood at room temperature overnight followed by drying in a vacuum oven at 50 °C for 24 h. After drying, the powder was weighed in a round-bottom flask and a solution of 0.8 M NaOH (aq) was added (10 mL solution per 1 g powder). The mixture was then put under stirring and reduced pressure to allow impregnation of the bark with the solution. Impregnation occurred for 10 min and was followed by hydrolysis under refluxing conditions. The reaction was stopped after 1 h and cooled to room temperature. The solid residue from birch bark powder was separated by centrifugation and the supernatant was acidified to pH 5.7 with 5 % H_2SO_4 (aq). The resulting precipitate was separated by centrifugation and then washed 4 times with de-ionized water/centrifugation cycles. Finally, the precipitate was recrystallized from toluene to yield EFA powder (yield: 60-70%)

3.4.1.2 Retrieval of epoxidized fatty methyl esters (e-FAMEs) from epoxidized linseed oil (ELO)

The transesterification of fatty methyl esters has previously been reported in the literature.[52] Following the literature procedure the e-FAMEs were obtained from transesterification by methanolysis. During a general procedure 20 g of ELO was weighed in a round-bottom flask containing a magnetic stir bar. A solution of 0.02 M NaOH dissolved in methanol was added to give a total volume of 250 mL. The reaction mixture was put under reflux conditions for 1 h then cooled to room temperature. The e-FAMEs were then extracted with 4x100 mL n-heptane. The organic phase was then dried with $MgSO_4$ (s) and filtered to remove the salt. Rotary evaporation was used in order to remove the n-heptane, resulting in the e-FAME mixture (yield: 75%). The monomers epoxy methyl oleate (EMO), epoxy methyl linoleate (EMLO) and epoxy methyl linolenate (EMLEN) were purified from the e-FAME mixture by automated column chromatography (Isolera 4, yields: EMO 10%, EMLO 11% and EMLEN 30%).

3.4.2 General procedure for the model studies performed

Table 5 shows a summary of the model studies performed. The experiments were made in order to investigate the different possible reaction pathways of the different thermosetting reactions. The experiments were based on two components (A and B) in a 1:1 molar ratio, carried out with or without catalyst. In addition, different reaction conditions were evaluated such as photo or thermal initiation. Moreover, different temperatures were evaluated for the thermally initiated reactions.

Table 5: Overview of the model studies performed. All reactants were based on a 1:1 molar ratio.

Comp. A	Comp. B	Reaction	Initiator	UV/T (°C)
LA	**LOH**	esterification	N/A	T: 120, 135, 150
EMO	**LA**	epoxy-acid	N/A	T: 120, 135, 150
EMO	**LOH**	transesterification/epoxy alcohol/epoxy-epoxy	N/A	T: 120, 135, 150
EMO	**LOH**	transesterification/epoxy alcohol/epoxy-epoxy	DDBSA	T: 130, 150, 170
EMLO	**LOH**	transesterification/epoxy alcohol/epoxy-epoxy	DDBSA	T: 130, 150, 170
EMLEN	**LOH**	transesterification/epoxy alcohol/epoxy-epoxy	DDBSA	T: 130, 150, 170

3.4.3 Synthesis of telechelic oligomers utilizing lipase catalysis

Table 6 shows an overview of the synthesized oligomers. Two different telechelic oligomers were synthesized utilizing immobilized *Candida antarctica* lipase-B (CALB, Novozyme 435) as a catalyst, one based on thiol-alkene and the other on thiol-epoxide. For a general synthetic procedure, monomers were added to a round bottom flask equipped with magnetic stir bars and set at 60 °C in oil bath. To the reaction mixture were added 10-15 wt% CALB of the total monomer amount.

Thiol-alkene oligomers were synthesized in bulk. The monomers, dimethyl succinate (DBE-4), *cis*-2-butene-1,4-diol and 6-mercapto-1-hexanol (MCh) were mixed under atmospheric pressure for 2 h before the reaction was left for 24 h under reduced pressure. The reaction was ended by adding acetone to the mixture and the enzyme was removed by filtration. Residual acetone was evaporated using a rotary evaporator. Three different targeted degrees of polymerization (DP) namely DP2, DP3 and DP4 were aimed. The products were used without further purification.

Thiol-epoxide oligomer was synthesized in toluene. The monomers, dimethyl adipate (DBE-6), EFA and 11-mercaptoundecanol (MUD) were mixed with toluene at 60 °C. Molecular sieves (4Å) were added in order to remove MeOH and H_2O. The reaction proceeded for 8 h and was stopped by adding $CHCl_3$ and removing the enzyme by filtration. Residual toluene solvent was removed by rotary evaporation. The product was used without further purification.

Table 6: Overview of the monomers used and the reaction conditions for the synthesis of telechelic oligomers.

Sample SH-Ene	Ratio[a] DBE-4:Diol:MCh	Time (T, p)[b]
DP2	3:2:2	2h (60°C, atm) -> 24h (60°C, 70mbar)
DP3	4:3:2	2h (60°C, atm) -> 24h (60°C, 70mbar)
DP4	5:4:2	2h (60°C, atm) -> 24h (60°C, 70mbar)

Sample SH-Epoxy	Ratio[a] DBE-6:EFA:MUD	Time (T, p)[b]
DP3	1:3:2	8h (60°C, atm)

[a] Molar ratio [b] Arrow "->" indicate change in condition during reaction.

3.4.4 Synthesis of diglycidyl furan-2,5-dicarboxylate (DGFDC)

Approximately 5 g of DAFDC was suspended in 40 mL dichloromethane with 11.8 g of 3-chloroperbenzoic acid (m-CPBA). The reaction conditions were set to 40 °C for 72 h, then the suspension was filtered and rinsed with 30 mL dichloromethane. The organic phase was then washed with 10% 50 mL Na_2SO_4 (aq), followed by 10% 50 mL Na_2CO_3 (aq) and finally 50 mL demineralized water. The organic phase was then dried with $MgSO_4$ (s), followed by filtration. The resulting solution was concentrated, yielding a white solid, diglycidyl furan-2,5-dicarboxylate (DGFDC, yield: 90%).

3.4.5 General procedures for the formation of polymer thermosets

Table 7 shows a summary of the different curing reactions and their respective conditions. The experiments have been divided into photo-initiated and thermally initiated cross-linking.

3.4.5.1 Photo-initiated cross-linking

For the photo-initiated cross-linking reactions of the telechelic oligomers, resin and initiator were dissolved in a vial with a small amount of $CHCl_3$. The sample was then casted on glass substrate, or directly on the crystal situated on the golden gate for RT-FTIR analysis. The solvent was allowed to evaporate before UV irradiation.

In the case of EMX-DGFDC/DGEBA the photo-initiation reaction occurred at 85 °C in order to avoid crystallization. For RT-FTIR analysis, samples with ratios of EMX:DGFDC (epoxy molar ratio ranging from 5:1 to 1:5) and initiator were dissolved in a vial with a small amount of acetone and vortexed to obtain a homogenous blend. The samples were then added to the preheated crystal on the golden gate and the solvent was allowed to evaporate before UV irradiation. For DMA analysis, the desired amount of EMX, DGFDC/DGEBA and initiator were added to a vial equipped with a magnetic stir bar. The vial was then closed and heated to 85 °C while stirring. The hot solution was then added to a preheated silicon or metal mold before UV irradiation.

3.4.5.2 Thermally initiated cross-linking

All thermally induced cross-linking reactions occurred in bulk. In the case of EFA, RT-FTIR was recorded for 3h and was started as soon as the sample was added to the preheated (150 °C) crystal situated on the golden gate. In the case of the FAME/e-FAME-polyester-melamine resin, the desired amount of FAME/e-FAME was mixed with polyester-melamine resin then spread on glass or steel substrates. The substrates were then put in the oven for 30 min. The reaction at 170 °C was followed by RT-FTIR.

The e-FAME-polyester/melamine resins were also cured in a simulated coil-coating environment resembling pilot-scale of the coil-coating process. The different formulations was cured on steel substrates for 30 seconds at 330 °C giving peak metal temperature (PMT) of 220 – 240 °C.

Table 7: Summary of the different cross-link reactions and their respective conditions.

Resin	Polymerization	Initiator	In wt%	UV/T (°C)
Thiol-alkene[a]	radical/step wise	Irgacure 651	4	UV
Thiol-epoxy[b]	cationic	UVAcure 1600	4	UV
EMX-DGFDC/ DGEBA[c]	cationic	UVAcure 1600	2	UV+T (85)
EFA[d]	esterification/epoxy-acid/epoxy-epoxy	EFA	N/A	T (150)
e-FAME-polyester/ melamine[e]	transesterification/epoxy -alcohol/epoxy-epoxy	DDBSA	3	T (130, 170)

[a] Paper I, [b] Paper II, [c] Paper III, [d] Paper IV and [e] Paper V

3.4.6 Post-modification procedure

The thiol-epoxy oligomer was cured on the surface of glass substrates. Two post-modification procedures were made. A catalytic amount of benzophenone (BPO) was added to the solutions containing a) 1,6-hexanediol mono vinyl ether (HMVE) (25 mg mL^{-1}) and b) heneicosafluorododecyl acrylate (25 mg mL^{-1}). Approximately 50 µL of each solution was spread on the glass substrates coated with thiol-epoxy thermoset. A quartz microscope slide was put on top of the sample before UV irradiation. UV-light exposure occurred for 20 min then the microscope slide was removed and the surface was washed three times with demineralized water. The glass substrate was left to dry in air.

4. Results and discussion

Herein the different epoxy based derivatives obtained from renewable resources and their applications as thermosets will be discussed. Epoxy fatty acid derivatives were isolated from naturally occurring raw materials. The purified monomers were either utilized as building-blocks in synthesis of oligomer resins which were subsequently cured, or used directly as monomers in thermosetting reactions. Finally the structure-property relationship was assessed for all obtained thermosets.

4.1 Epoxy functional fatty acid derivatives from renewable resources

The topic of this thesis is polymer materials from renewable resources therefore the choice of raw materials for the retrieval of monomers was made in order to be as sustainable as possible. In the context of polymer materials for coating applications, epoxy functional monomers or oligomers have been used for many decades.[90] For instance, it is hard not to think about "epoxy glue" when you hear the word adhesive. As earlier mentioned, the functional group is interesting due to the inherent ring-strain enabling reactivity in both basic and acidic conditions.

4.1.1 Retrieval of 9,10-epoxy-18-hydroxyoctadecaonic acid (EFA)

The land area of Sweden is largely based on forest.[118] The forestry industry accounts for a large share of the exports of the country.[119] During the production of forestry products side streams are often produced. In the case of both pulp and paper mills and saw mills the first step is debarking of the trees, generating a side stream considered to have low inherent value.[35] In the case of birch tree bark, previous studies have shown that it is possible to retrieve fatty acid derivatives from the suberin macromolecular polyester structures.[24,32,34,36,33] Hence, birch tree bark was utilized as a raw material in the extraction of EFA. The EFA is interesting due to the three different functional groups. With hydroxyl, carboxylic acid and epoxide groups all residing in the same molecule, EFA enables many possible chemical reactions. EFA was extracted by cleaving the ester bonds in suberin in basic conditions of NaOH (aq) followed by precipitation through lowering the pH to 5.7. Pure EFA (s, Figure 7) was obtained from recrystallization in toluene with a yield of 60-70 %. Recrystallization from isopropanol resulted in lower yields. In addition, lowering the pH below 5.5 resulted in ring-opening, forming 9,10,18-trihydroxyoctadecanoic acid[32] and the yield of the epoxide decreased significantly.

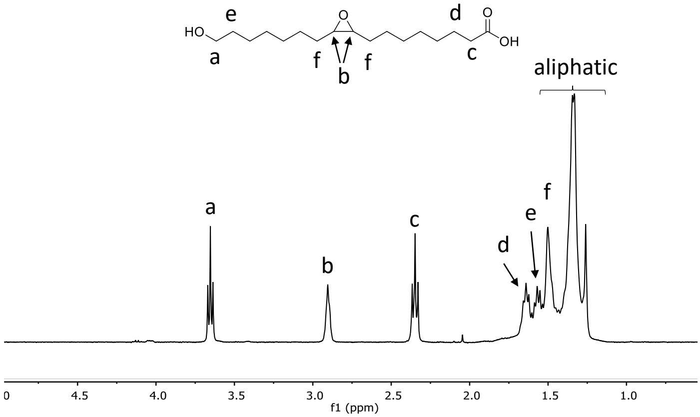

Figure 7: ^{1}H NMR ($CDCl_3$) spectrum of EFA extracted from outer birch bark.

4.1.2 Retrieval of the epoxidized fatty methyl esters (e-FAMEs)

In the case of the e-FAMEs, epoxidized linseed oil was used as raw material. The ester bonds within the triglyceride were cleaved by basic conditions of NaOH in methanol. The NaOH in methanol was chosen over NaOH (aq) in order to obtain methyl esters instead of acids. This was done mainly for purification reasons. Acids are known to interact with silica particles and are therefore more challenging to purify. After the reaction the crude mixture was exposed to solvent extraction in n-heptane to separate e-FAMEs from glycerol. The yield of e-FAMEs was 75 %. The different fatty compounds within the e-FAME mixture were purified by automatic column chromatography using silica particles as the stationary phase and a gradient of n-heptane/EtOAc as the mobile phase. A TLC study in n-heptane/EtOAc showed that 4 products were present in the e-FAME mixture, which after purification were verified by NMR (Figure 8) and FTIR (Figure 9) to be methyl stearate, EMO (yield 10 %), EMLO (yield 11 %) and EMLEN (yield 30 %). The first product (methyl stearate) was not used and it is therefore not discussed further.

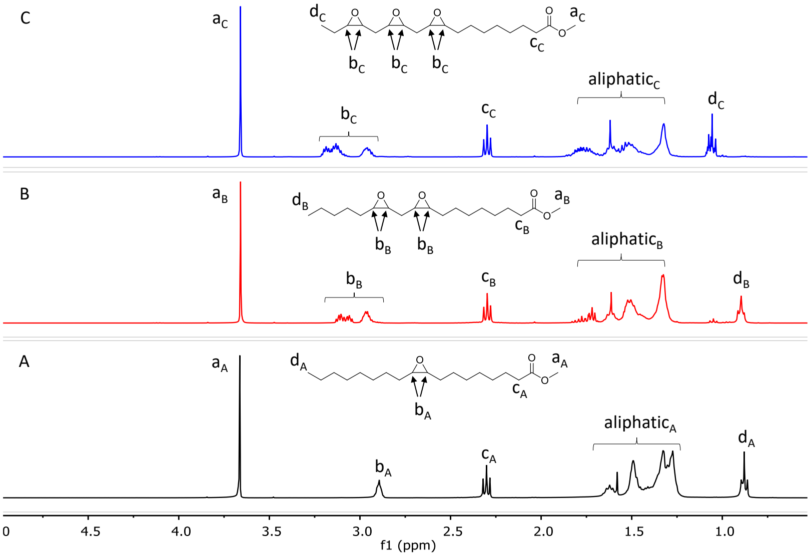

Figure 8: ${}^{1}H$ NMR ($CDCl_3$) spectra of (A) EMO (B) EMLO and (C) EMLEN extracted from epoxidized linseed oil.

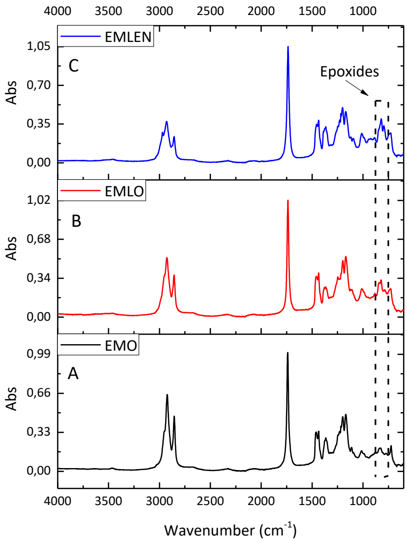

Figure 9: FTIR of (A) EMO, (B) EMLO and (C) EMLEN extracted from epoxidized linseed oil.

4.2 Multifunctional aliphatic oligomers synthesized by enzymatic catalysis (Paper I and Paper II)

The purpose of this section is to demonstrate more benign routes in polymer synthesis. Lipase catalysis was used in order to synthesize multifunctional molecules which are difficult to synthesize using traditional polymer chemistry. Functional groups such as thiols, alkenes and epoxides were interesting to add in the resin structures. Conventional synthesis protocols of thiol functional polymers rely on protection and deprotection chemistry due to the instability of the thiol group.[73–75] The use of such protocols shows that it is possible to functionalize molecules with thiols however, the processes are tedious and include many steps. A few examples have been reported on thiol functionalized polymers synthesized in one-pot reactions without protection and deprotection using e.g. $Sc(OTf)_3$ or HCl as catalysts.[120,121] Another way to overcome the tedious protocols is to use enzyme catalysis. Enzymes display high selectivity and operate in mild reaction conditions. The catalysts can perform in solvent or bulk and they can be recycled several times.[79,80] These features provide an environmentally friendly platform in the synthesis of novel multifunctional polymers. The synthesis of multifunctional aliphatic oligomers and their ability to form thermosets are discussed herein.

4.2.1 Synthesis of multifunctional aliphatic oligomers

Lipases, a class of enzymes, are highly efficient in forming esters under mild conditions.[69,80] For instance the chemo-selectivity of *Candida Antarctica* lipase-B (CALB) is almost 10^5 times higher towards alcohol than thiol in transacylation reactions.[83] In previous attempts, immobilized CALB has successfully been applied in the synthesis of novel linear multifunctional oligomers without harming reactive functional groups such as oxetanes, alkenes or epoxides.[84,85,122] In the pursuit of synthesizing oligomers without harming the epoxide, thiol or alkene, lipase catalysis was therefore a suitable approach. Two different oligomers were synthesized, both with thiol end-groups but varying the functionality of the repeating unit with either alkene or epoxide, using immobilized CALB.

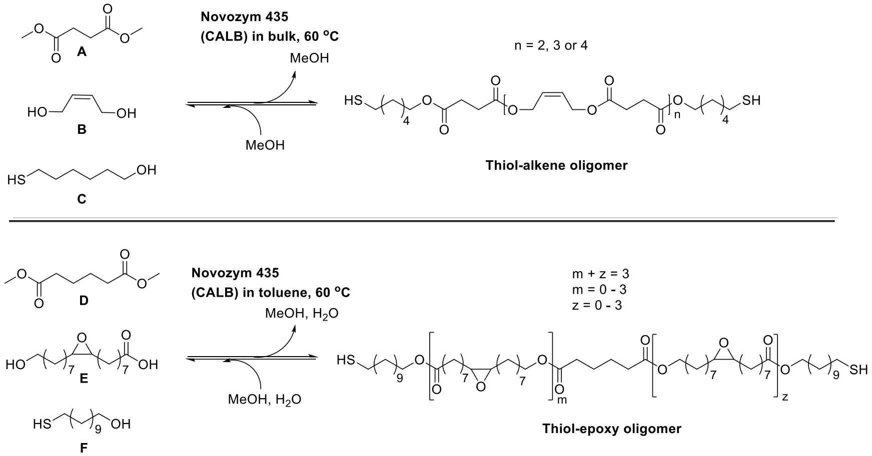

Scheme 3: Synthetic scheme of the telechelic oligomers. Above shows thiol-alkene and below shows thiol-epoxy.

Due to the enzymatic catalysis being an equilibrium reaction, a key aspect in pushing the reaction forward was the removal of formed by-products[78,123] which was resolved by adding molecular sieves or applying vacuum. Both oligomers (thiol-alkene and thiol-epoxy) were obtained by one-pot condensation reactions under mild conditions using immobilized CALB as a catalyst (Scheme 3). Thiol-alkene oligomer was synthesized in bulk conditions however, in the case of thiol-epoxy, toluene as a solvent was required to obtain a homogenous blend at set reaction temperature. The obtained DP and M_n were both in line with the theoretically calculated values (Table 8), thus potential coupling reactions such as disulphides, thiol-ene coupling or thiol-epoxy coupling were negligible. Large molecular weight distributions were however obtained as shown from Đ values. NMR (Figure 10) confirmed the synthesis by the formation characteristic ester peak (4.10 ppm). In addition, the different functionalities i.e. thiol (2.54 ppm) and alkene (4.70 and 5.74 ppm) or epoxide (2.90 ppm) were intact after the reaction thus confirming the selectivity of the enzyme. However, a very small amount of thioester (2.88 ppm) could be detected in the thiol-alkene oligomer.

In the case of the thiol-epoxy oligomer MALDI-TOF-MS analysis (Figure 11) showed that the mass difference between the peaks was 296 Da, corresponding to a EFA-repeating unit. The analysis further revealed that there were two families of chemical structures: one bi-functionalized with thiols on both ends and the other mono-functionalized. A reasoning to this outcome could be the monomer EFA having a carboxylic acid and a hydroxyl as end-groups, thus rendering the possibility of self-condensation simultaneously as end-capping of EFA.

Control reactions without enzyme under similar conditions resulted in no observable reactions. Experiments at elevated temperatures of 120 °C (for thiol-alkene oligomer) and 85 °C (for thiol-epoxy oligomer) both resulted in insoluble networks, thereby confirming the complexity of mixing the functionalities without adding CALB.

The possibility of synthesizing the oligomers without harming functionality of interest further show the advantage of utilizing enzyme catalysis. Due to the selectivity of the enzyme it was possible to mix the reactants and obtain multifunctional aliphatic oligomers from one-pot reactions.

Table 8: Overview of the synthesized telechelic oligomers and the respective thermoset properties. Thiol-alkene (SH-ene) oligomers are shown in the top part of the table while thiol-epoxy (SH-Epoxy) is shown in the bottom part of the table.

	Oligomer resins					**Thermosets**	
Sample SH-Ene	**DP**[a]	**Ratio A:B:C**	f_{SH}[b] **(%)**[a]	**M_n (g mol^{-1})**[c]	**Đ**[c]	**T_g (°C)**[d]	**G' (MPa)**[e]
DP2	1.9	3:2:2	82	670	2.0	-15	1.4
DP3	2.9	4:3:2	85	970	2.6	-18	0.4
DP4	3.7	5:4:2	82	1020	2.1	-20	0.2

Sample SH-Epoxy	**DP**[a]	**Ratio D:E:F**	f_{SH}[b] **(%)**[a]	**M_n (g mol^{-1})**[c]	**Đ**[c]	**T_g (°C)**[d]	**G' (MPa)**
DP3	2.5	1:3:2	98	1190	2.5	N/A	N/A

[a] Determined by ^{1}H-NMR; [b] Degree of thiol functionalization; [c] Determined by SEC [d] T_g property of thermoset, determined from the second heating on DSC [e] Shear modulus of thermoset, determined from rheology

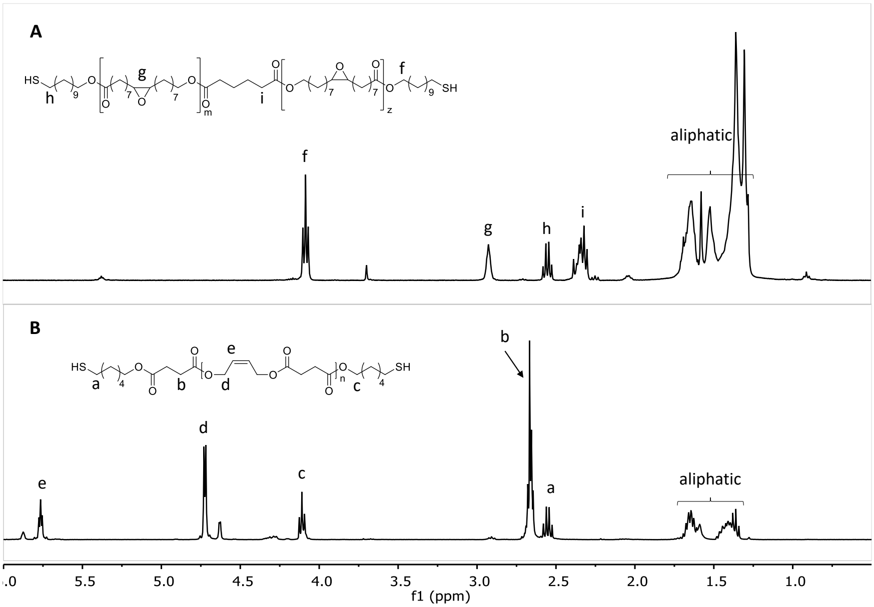

Figure 10: ^{1}H-NMR ($CDCl_3$) of the synthesized telechelic oligomers. (A) Shows thiol-epoxy and (B) shows thiol-alkene.

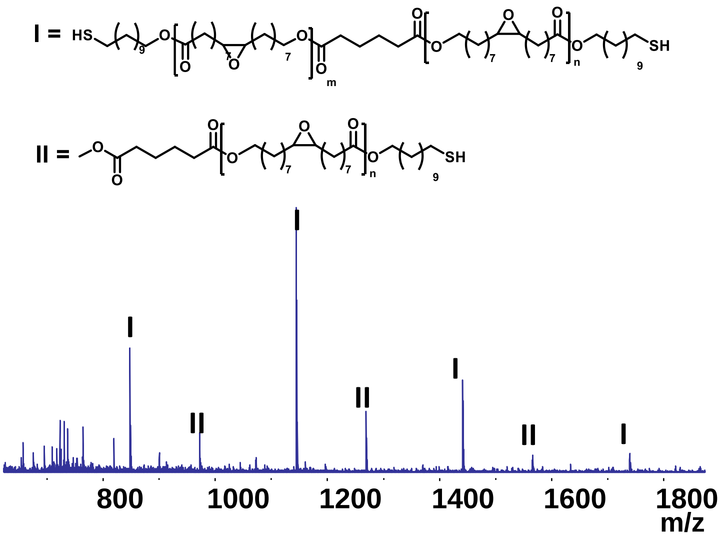

Figure 11: MALDI-TOF-MS of thiol-epoxy oligomer showing 2 families: one with di-end thiol and one with mono-end thiol.

4.2.2 Thermosets from multifunctional linear aliphatic oligomers

The presence of 2 or more different functional groups rendered in several possible routes of forming polymer network. One example was to utilize the oligomers as a one-component resin. Another example was to form thermosets with post-functionalization possibilities. One component resins, thiol-alkene and thiol-epoxy multifunctional aliphatic oligomers, were obtained by lipase catalysis in a one-pot reaction. Both oligomers were exposed to UV-light while following the polymer network formation by RT-FTIR analysis.

In the case of thiol-alkene, UV irradiation resulted in a thiol-ene coupling reaction (Figure 12a). Increased DP resulted in "left-over" *trans*-alkene within the polymer network (Figure 12b). Additionally, decreases in both T_g and mechanical properties were observed with increased DP (Table 8).

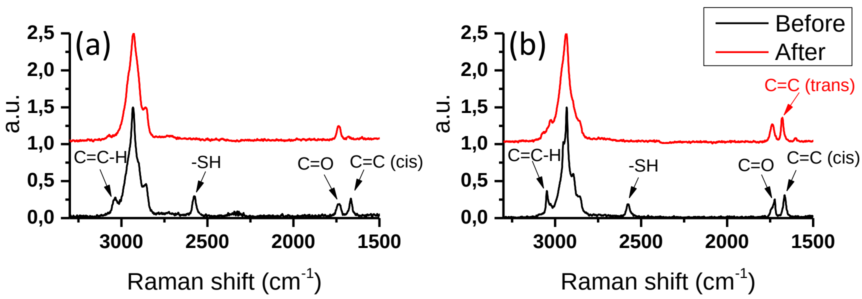

Figure 12: Curing of thiol-alkene oligomer, FT-Raman results. (a) Shows DP2 and (b) shows DP4.

In the case of the thiol-epoxy oligomer, the epoxides were cross-linked by cationic polymerization as shown from RT-FTIR (Figure 13b) yielding a soft thermoset at room temperature. The thiol groups were unharmed, as evidenced by FT-Raman (Figure 13a). It was uncertain if the thiols were available on the surface of the coating for post-modification, however it is known that thiols undergo thiol-ene coupling effectively.[88] As a proof-of-concept two attempts at modifying the surface via thiol-ene coupling were chosen: hydrophilic by 1,6-Hexanediol mono vinyl ether (HMVE) and hydrophobic by heneicosafluorododecyl acrylate (HFA). Additionally, benzophenone (BPO), a hydrogen abstracting initiator, was chosen. The hypothesis was to enable thiyl radical formation from surface thiols and thereby limiting homo-polymerization of HMVE and HFA respectively. Figure 14 shows contact angle measurements of non-modified (60°) and the two different modifications of the surface: hydrophilic (30°) and hydrophobic (130°). This indicated that thiols were available on the surface for post-modification as compared to the initial thiol functional surface.

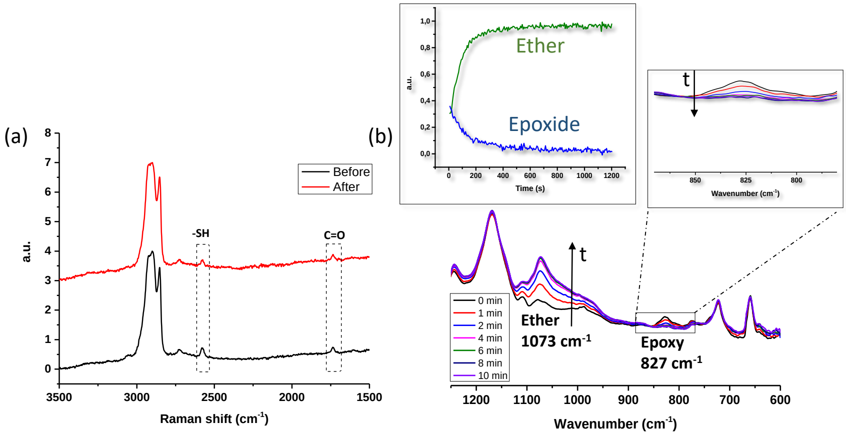

Figure 13: Curing of thiol-epoxy oligomer. (a) Shows FT-Raman and (b) RT-FTIR of cationic curing of epoxides.

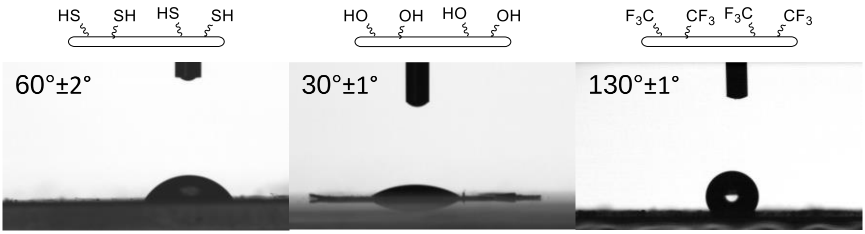

Figure 14: Contact angle of water droplets on surface cured thiol-epoxy oligomer. To the left, no modification after curing. In the middle, post-modification of surface by reacting HMVE with thiols on surface i.e. changing the surface from –SH to –OH (published). To the right (unpublished result), post-modification of surface by reacting HFA with thiols on surface i.e. changing surface from –SH to –CF_3.

4.3 Introducing a bio-based rigid component to epoxy based fatty methyl esters (Paper III)

Purely aliphatic fatty acid derivatives yield low T_g thermosets, which is normally addressed by introducing aromatic structures such as diglycidyl ether of bisphenol-A (DGEBA). DGEBA is an aromatic, rigid, colorless organic compound often used in epoxy resin formulations. While DGEBA is recognized as one of the most used monomers in different coating applications,[90] it is however a made from petrochemical feedstock. Herein an alternative approach to thermosets made from DGEBA are discussed. The US Department of Energy (US DOE)[124] has identified FDCA as one of the most promising building-blocks for the renewable chemical industry. FDCA is a rigid organic compound resembling aromatic character that can be obtained from 5-hydroxymethylfurfuraldehyde (HMF), which in turn is derived from sugars.[10] The process of obtaining FDCA has been expensive and not feasible on a commercial scale, until recent advances made by Avantium.[125] The chemical structure of FDCA is similar to aromatic monomers obtained from fossil resources hence, it represents a sustainable alternative in the manufacturing of polyesters, polyamides and polyurethanes. Continuing on the theme of epoxy functional monomers from renewable resources, the approach was to extend FDCA into epoxy thermoset applications.

4.3.1 Synthesis of diglycidyl 2,5-furandicarboxylate (DGFDC)

In an effort to explore FDCA as a suitable alternative to DGEBA, epoxidation of FDCA was performed. At our disposal we had diallyl furan-2,5-dicarboxylate (DAFDC) synthesized from a sustainable protocol.[116] In order to continue with the sustainable theme of the thesis, an approach exploring a sustainable route in the epoxidation of DAFDC was assessed. Double bonds have previously been epoxidized in the presence of CALB, hydrogen peroxide and an organic carboxylic acid.[57,58]

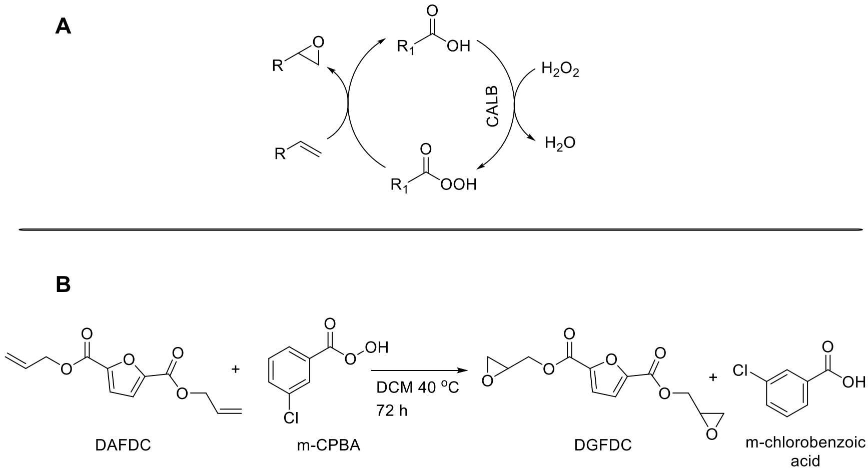

Scheme 4: Epoxidation routes of DAFDC. (A) Shows epoxidation by CALB and (B) shows epoxidation by *m*-CPBA.

Björkling et al[57,58] showed that the role of CALB was to generate peroxycarboxylic acids from the parent organic carboxylic acid and hydrogen peroxide. The peroxycarboxylic acid subsequently epoxidized the alkene (Scheme 4A). In the attempt to epoxidize DAFDC using immobilized CALB and hydrogen peroxide different protocols were examined. NMR analysis in DMSO-d_6 (Figure 15A) provided a means for following the epoxidation. Protons on the furan ring (7.46 ppm) gave rise to a new peaks downfield depending on if DAFDC was mono- or di-functionalized. The best outcome in epoxide conversion was obtained using 20 wt% CALB with octanoic acid, which resulted in 45% conversion of a mixture of mono- and di-epoxides after 50 h reaction time (Figure 15B). It was however challenging to purify the DGFDC from the mixture. Adding buffer (K_2HPO_4) did not improve the epoxidation results neither did extending the time to 72 h.

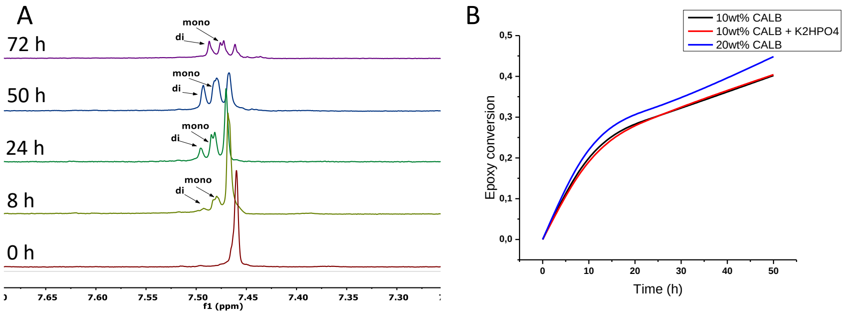

Figure 15: (A) shows [1]H NMR (DMSO-d_6) from the 20wt% CALB epoxidation reaction. (B) shows epoxy conversion utilizing different CALB epoxidation experiment setup.

Due to the CALB approach not being feasible in our approach, other means in epoxidizing DAFDC were assessed in order to continue with the study. A commonly used epoxidation method is the Prileschajew reaction,[126] which uses a peroxide in order to epoxidize an alkene. A commonly used peroxide is *m*-CPBA.[127–129] Using *m*-CPBA procedure (Scheme 4B) resulted in DGFDC with 90% yield (Figure 16). However, in order to keep the process as environmentally friendly as possible one should recycle the waste i.e. dichloromethane and *m*-chlorobenzoic acid for other reactions.

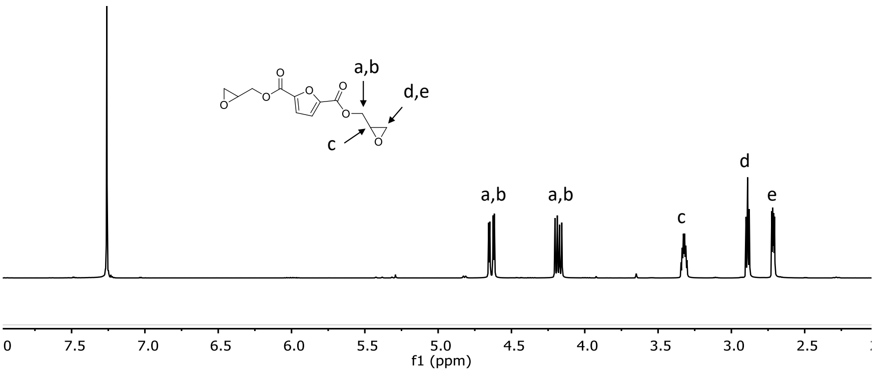

Figure 16: [1]H NMR ($CDCl_3$) of DGFDC.

4.3.2 Bio-based UV-cured epoxy thermosets

The underlying idea of synthesizing diglycidyl furan-2,5-dicarboxylate (DGFDC) was to introduce a rigid component from renewable resources to our "toolbox" for the formation of polymer networks. The telechelic oligomers provided versatility in surface modification, however the formed thermosets were applicable as soft T_g materials. DGFDC, being a rigid compound, yields a brittle thermoset if cross-linked alone. It is known that epoxides cross-link well when utilizing cationic polymerization.[92,94,105] Pure epoxidized fatty methyl esters (EMX); EMO, EMLO and EMLEN which were retrieved from ELO could act as "plasticizers" if cross-linked with DGFDC. First, the co-polymerization of the monomers DGFDC and respective EMX-monomer were confirmed utilizing UVAcure 1600 as an initiator in reactive DSC. It has previously been shown that cationic UV-initiators can thermally decompose and initiate reactions similar to those of UV-initiated processes[130] hence, the results can be comparable. Reactive DSC of pure monomers i.e. DGFDC, EMO, EMLO and EMLEN revealed that a lower activation energy was needed for the homo-polymerization of the EMX monomers in comparison to DGFDC (Figure 17a). Similarly reactive DSC experiments were carried out utilizing a mixture of 1:1 epoxy ratio of EMX:DGFDC. All experiments yielded a co-polymerization indicated by the one combined curing peak occurring at lower temperature than needed for pure DGFDC monomer and higher than pure EMO monomer (Figure 17b).

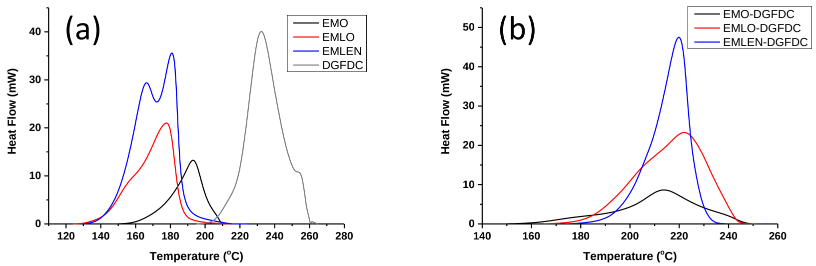

Figure 17: Reactive DSC scans on (a) monomers EMO, EMLO, EMLEN and DGFDC (b) mixture 1:1 epoxy molar ratio of EMO:DGFDC, EMLO:DGFDC and EMLEN:DGFDC.

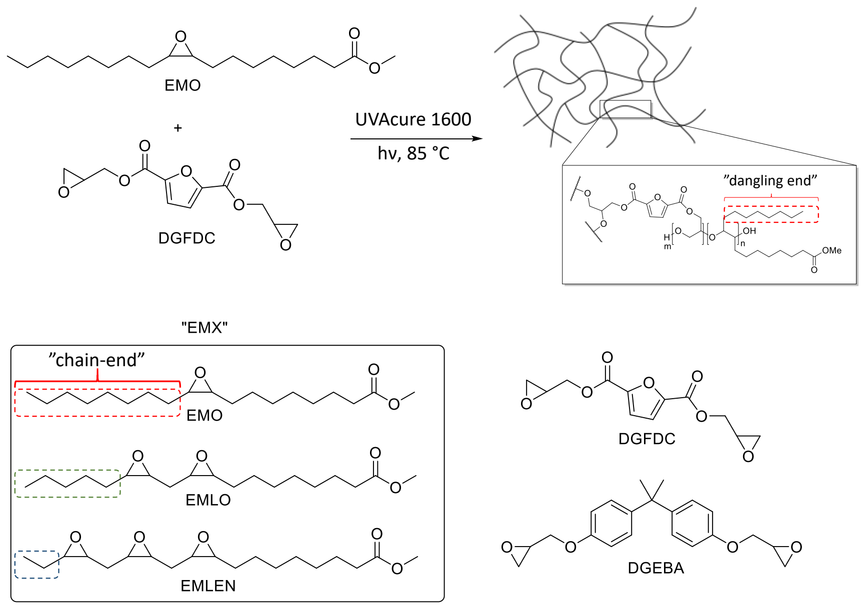

Figure 18: The EMX, DGFDC and DGEBA monomers used and the network formation of the UV-initiated reaction between EMO and DGFDC.

Knowing that the monomers were able to co-polymerize, it was possible to continue with UV-initiated curing. The UV-initiated curing was followed by RT-FTIR. Pure monomers and mixture of EMX:DGFDC ranging from 5:1 to 1:5 (epoxy molar ratio) were studied. Relative curing profiles were determined by following the formation of ether bonds (1150 – 1060 cm^{-1}) correlated to the disappearance of the epoxide ring-vibration (950 – 750 cm^{-1}). It should be noted that the peaks reside in the fingerprint region which created an obstacle in calculating conversions with high accuracy. Due to the obstacle of not being based on clearly isolated absorbance peaks, all results are relative between initial and final states and should be considered as trends. To further clarify this, 100% conversion represents the point at which no changes in the ether region were observed. Figure 19 shows the formation of ether bonds from the obtained results from RT-FTIR. The reactions of the pure monomers followed by RT-FTIR (Figure 19a) revealed that curing of EMO was the fastest followed by EMLO then EMLEN. All EMX monomers were much faster than DGFDC thus resembling reactive DSC results. Figure 19b, c and d show the results from reaction of DGFDC with

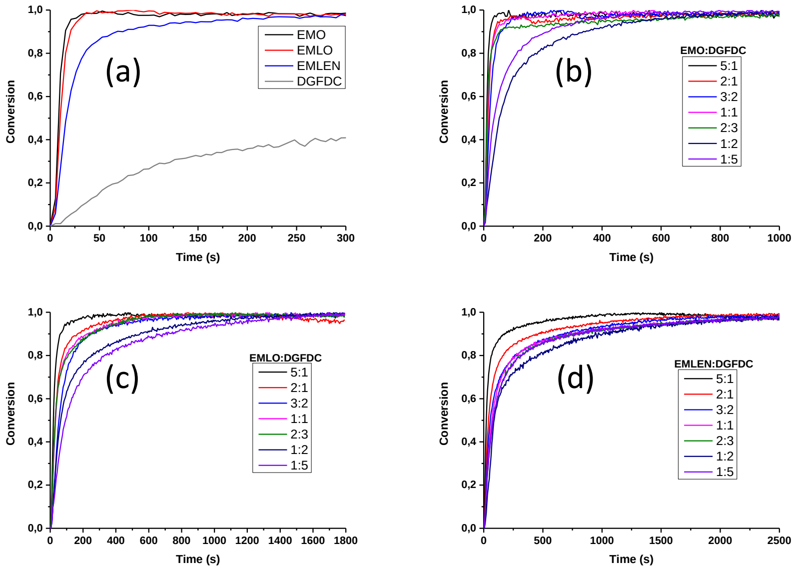

Figure 19: RT-FTIR on photo-curing of (a) monomers EMO, EMLO, EMLEN and DGFDC, (b) EMO-DGFDC system, (c) EMLO-DGFDC system and (d) EMLEN-DGFDC system. Showing normalized conversion of the ether bond absorbance peak.

EMO, EMLO and EMLEN respectively. Adding DGFDC to the pure EMX resulted in a decrease in the conversion rate of all systems. Furthermore, the effect of the epoxy functionality was also evaluated, revealing that higher functionality correlates with longer conversion times. Both by adding the rigid component (DGFDC) and increased functionality on EMX suggests limitation in "free movement" within the formed network.

DMTA analysis was made on networks from EMLO-DGFDC and EMLEN-DGFDC in order to evaluate the influence of DGFDC and EMX on the final network properties. Table 9 shows the results obtained from DMTA analysis and Figure 20 shows the obtained graphs of storage modulus (E') or tan δ vs temperature. Introducing DGFDC resulted in material exhibiting a T_g ranging from 0 °C up to 100 °C. With an increasing amount of DGFDC in the EMLO-DGFDC system, a higher T_g and E' were obtained. As expected, the rigid structure of DGFDC provided thermal and mechanical stability. In addition, an increased amount of DGFDC yielded higher cross-link density which may be a contribution to the limitation in the "free movement" earlier suggested. Introducing an extra epoxide on the fatty acid, i.e. going from EMLO to EMLEN, had a clear impact on the final network properties yielding significantly higher T_g and E' values at room temperature. This may be a contribution from the amount of "dangling ends" formed in the cross-linked network. EMLO, having longer chain-end, yields less limitations in the movement, which results in a lower T_g. The trend regarding "dangling ends" has previously been described in literature,[51] the results from which resemble those obtained from our experiments. However, increasing the functionality on the EMX results in a less homogenous network as noticed from the broadening effect on the tan δ curve. Moreover, an extra epoxide provides an extra cross-link point; hence, a higher cross-link density was observed. Changing DGFDC to DGEBA in the EMLO system resulted in higher T_g, E' (at 20 °C) and cross-link density (Table 9). The increased T_g and E' (at 20 °C) obtained was a result of DGEBA containing 2 aromatic rings in the structure, which enabled more rigidity. However, higher cross-link densities are harder to explain directly. One can speculate that the epoxides of DGEBA have higher reactivity which would render in more DGEBA reacting into the final material.

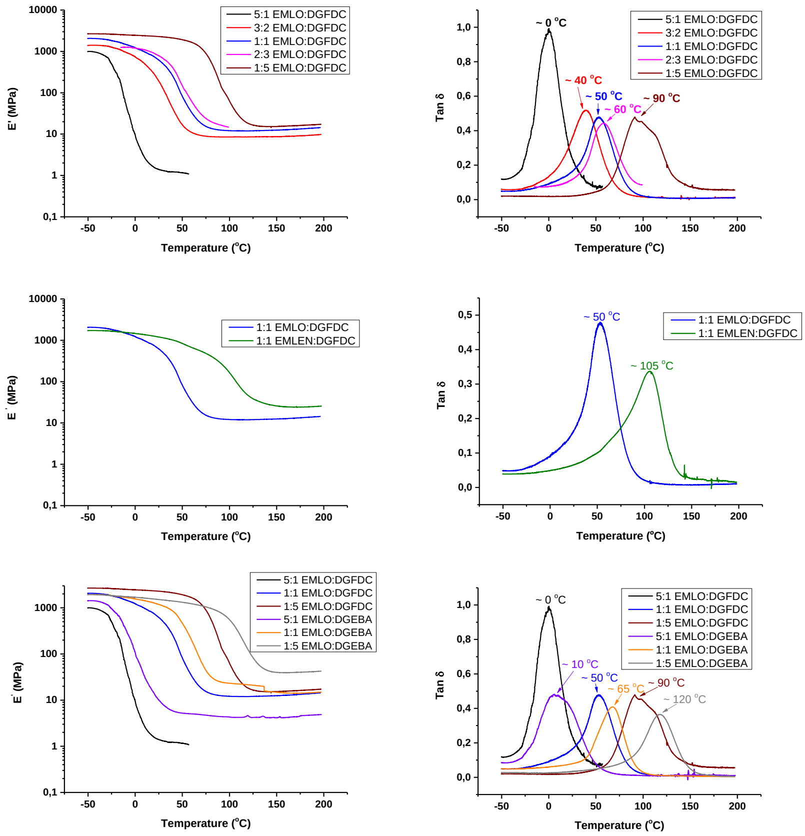

Figure 20: DMTA analysis showing thermal and mechanical properties of the obtained thermosets. (A-B) shows EMLO-DGFDC system, (C-D) shows comparison of EMLO:DGFDC with EMLEN:DGFDC both 1:1 epoxy molar ratio, (E-F) shows comparison of EMLO:DGFDC with EMLO:DGEBA both 1:1 epoxy molar ratio.

Table 9: Thermal and mechanical properties of the thermosets.

Sample EMLO:DGFDC	T_g(°C)[a]	E'(20°C) (MPa)	$E'_{rubbery}$ (MPa)	ν_e (mol m^{-3})
5:1	1	1,6	1	130
3:2	40	290	9	820
1:1	50	750	13	1200
2:3	60	900	14	1500
1:5	90	2300	17	1600

Sample EMLEN:DGFDC	T_g(°C)[a]	E'(20°C) (MPa)	$E'_{rubbery}$ (MPa)	ν_e (mol m^{-3})
1:1	105	1300	26	2400

Sample EMLO:DGEBA	T_g(°C)[a]	E'(20°C) (MPa)	$E'_{rubbery}$ (MPa)	ν_e (mol m^{-3})
5:1	9	10	39	600
1:1	70	1300	22	2200
1:5	120	1600	5	3700

[a] T_g value obtained from optimum of tan δ curve

4.4 Thermosets from EFA through self-condensation (Paper IV)

After a long day following the extraction procedure of EFA it was forgotten in a vial in a vacuum oven at 50 °C overnight, resulting in an insoluble network. Of course we were curious of what happened overnight so we set up model experiments in an attempt to evaluate the different reaction pathways of EFA at elevated temperatures (Table 10). As mentioned earlier, EFA contains a hydroxyl group, an epoxide and a carboxylic acid.

Table 10: Model experiments performed in order to evaluate the possible reaction pathways of EFA at elevated temperatures.

Comp. A	Comp. B	Reaction	Catalyst	T (°C)
LA	**LOH**	esterification	N/A	T: 120, 135, 150
EMO	**LA**	epoxy-acid	N/A	T: 120, 135, 150
EMO	**LOH**	transesterification/epoxy alcohol/epoxy-epoxy	N/A	T: 120, 135, 150
EMO LA LOH		competing reaction of above mentioned	N/A	T: 120, 135, 150

For the model experiments an aliphatic alcohol (Lauryl alcohol (LOH)), corresponding acid (Lauryl acid (LA)) and EMO were chosen as model compounds. The compounds were chosen for miscibility reasons and mixed in a 1:1 molar ratio. EMO was chosen due to its structural similarity to EFA. No catalyst was added and the reactions were followed by RT-FTIR and NMR (before and after). The results from the model experiments can be seen in Figure 21.

The esterification reaction between LA and LOH occurred at all temperatures. The shift from acid (1715 cm^{-1}) to ester (1740 cm^{-1}) reached approximately 70% conversion after 2 h at 150 °C.

The epoxy-acid reaction was identified by the disappearance of the acid signal (1715 cm^{-1}). A small decrease in the epoxide region (approx. 830-820 cm^{-1}) was also observed; however, the absorption band overlapped with other peaks in the fingerprint region. The reaction from epoxy-acid would

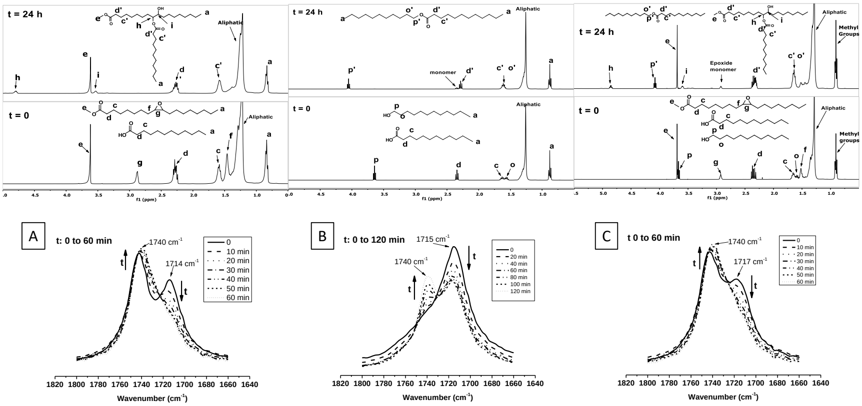

Figure 21: Model experiments performed, ^{1}H-NMR on top and RT-FTIR on bottom. (A) shows reaction between EMO-LA, (B) shows reaction between LA-LOH and (C) shows reaction between EMO-LA-LOH.

generate an alcohol and an ester this was confirmed by RT-FTIR from an increase in absorbance from respective region, alcohol at 3530 cm^{-1} and ester at 1740 cm^{-1}. The reaction reached 90% conversion after 40 min at 150 °C, which was faster than the direct esterification reaction of LA and LOH. In addition, it should be noted that a small increase was also observed in the linear aliphatic ether region (1150-1060 cm^{-1}), indicating a reaction between epoxide-epoxide.

No reactions were observed from the EMO-LOH experiment. LOH was deemed to be not nucleophilic enough on an inactivated secondary epoxide of EMO. A transesterification did not occur either.

The competing reactions when using all compounds (EMO LA LOH) showed a similar trend to the above mentioned reactions. The results obtained suggest that the acid may be the catalyst in the process protonating the epoxide. Different types of reaction were then possible on the protonated epoxide, namely acid-epoxide ring-opening, alcohol-epoxide ring-opening, epoxide-epoxide ring-opening. Furthermore, direct esterification was also possible; however, model experiments showed that it was slower, hence the esterification should be formed to a less extent.

Finally, the reaction of EFA at 150 °C was followed by RT-FTIR and NMR (Figure 22). The reaction displayed a similar trend to the model experiments. Acid and epoxide absorbance peaks decreased while ester, alcohol and linear aliphatic ether increased. After approximately 40-50 min a glue like material was obtained. Figure 23 show two different substrates glued by heating EFA.

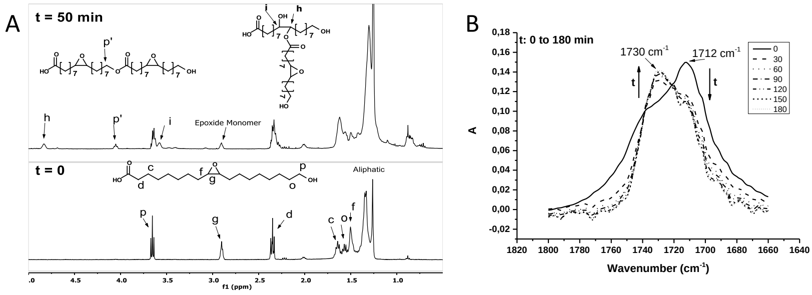

Figure 22: Curing of EFA at 150 °C. (A) shows [1]H-NMR before gelation and (B) shows RT-FTIR.

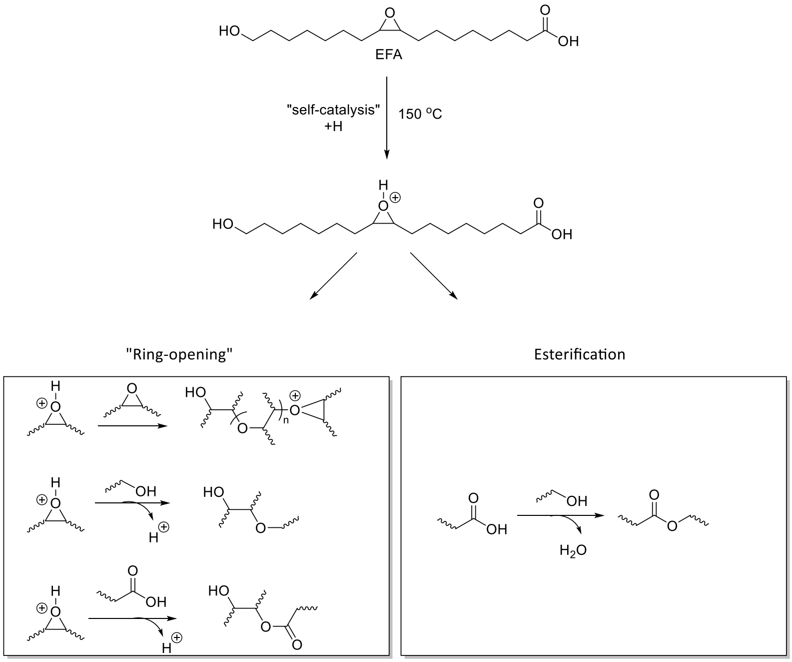

Scheme 5: Suggested reaction scheme for EFA curing at 150 °C.

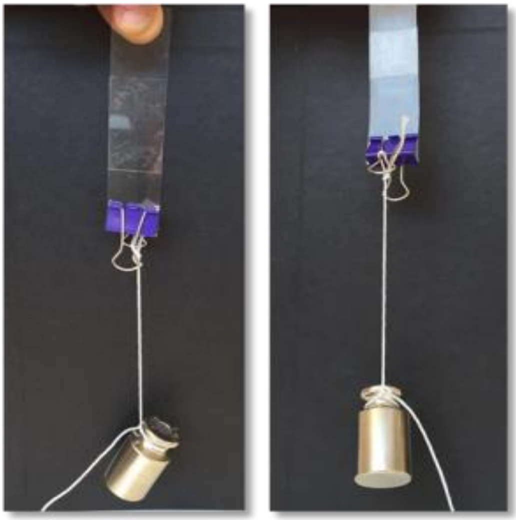

Figure 23: Glue-like property of cured EFA.

4.5 Coil-coatings using epoxidized fatty acid derivatives (Paper V)

Fatty acid derivatives have a long history in coating applications. One of the first uses of fatty acids in coating applications was in alkyds, as early as the 19th century.[15] The fatty acids were used in order to add flexibility to the alkyd as well as to allow an oxidative drying. More recently, fatty acid derivatives have been used as monomers and reactive diluents in coil-coatings.[115] In traditional coil-coatings the formulation is a solvent-borne liquid in order to attain the desired flow properties. The formulation is applied on a substrate, such as steel, and chemically cross-linked in high temperature convection ovens.[47,111] During the process, a vast amount of volatile organic compounds (VOCs) are evolved.[47] One way to avoid VOCs in the formulation is to add a reactive diluent which is a molecule that retains the flow in the formulation and reacts into the final network upon curing.[112] Fatty acid methyl esters (FAMEs) have previously been used as renewable reactive diluents in polyester-melamine coil-coatings formulations in order to reduce VOCs as well as making the coating partly bio-based.[112] The studies reveal that FAMEs are incorporated into the final network. However, since the curing occurs at high temperatures, loss of FAMEs due to evaporation also occurred. We hypothesized that epoxide groups residing in the e-FAME structure would increase incorporation in the final coating in comparison to FAME.

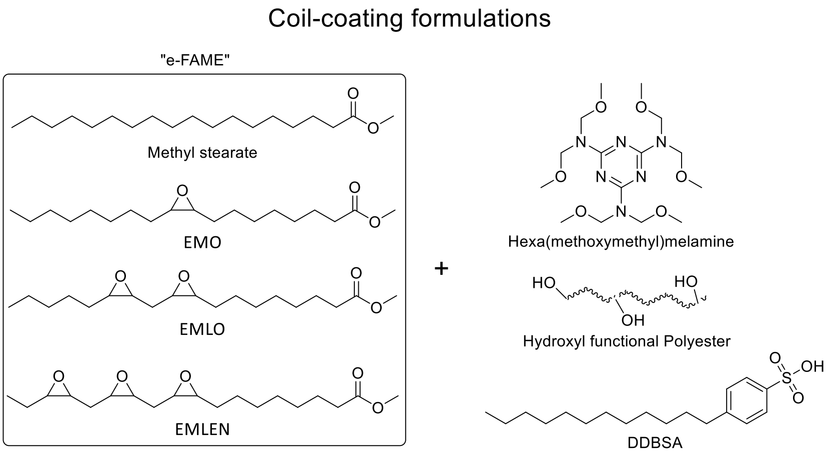

Figure 24: Coil-coating formulations evaluated in this thesis project.

In a proof-of-concept effort the e-FAMEs were applied in polyester/melamine coil-coatings formulations in order to increase their incorporation in the dry coating in comparison to FAMEs. As earlier mentioned, a reactive diluent should have a diluting effect while reacting into the final network upon curing. Rheology measurements confirmed that increasing amount of e-FAME had a diluting effect on the polyester-melamine resin mixture as seen in Figure 25.

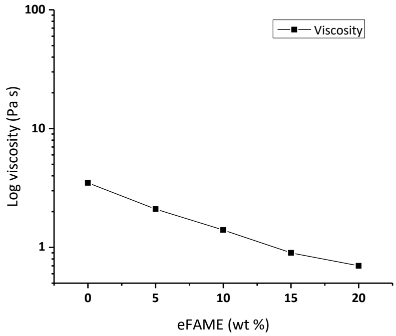

Figure 25: The viscosity of polyester-melamine resin containing an increasing content of e-FAME.

Table 11: Model experiments to investigate possible reactions of coil-coating formulations.

Sample	Reaction	Initiator	T (°C)
EMO-LOH	transesterification/epoxy alcohol/epoxy-epoxy	DDBSA	T: 130, 150, 170
EMLO-LOH	transesterification/epoxy alcohol/epoxy-epoxy	DDBSA	T: 130, 150, 170
EMLEN-LOH	transesterification/epoxy alcohol/epoxy-epoxy	DDBSA	T: 130, 150, 170

The intended coil-coating formulation would have epoxides, alcohols (from polyester) and methyl esters/ethers from e-FAME and melamine respectively. Model experiments (Table 11) were setup to investigate the possible reactions that could occur. EMO, EMLO or EMLEN were mixed with LOH in a 1:1 molar ratio. The different reactions were then followed by RT-FTIR at 130 °C, 150 °C and 170 °C. The results are presented in Figure 26. The different profiles (ester, ether, epoxide and OH) represent the area under the curve over time of respective absorbance peak measured on RT-

FTIR. Similar obstacle to Paper III was encountered regarding no clearly isolated peaks in fingerprint region for ether and epoxide absorbance peaks. The RT-FTIR data should thus be considered as trends and rather than absolute values.

A qualitative comparison was made between the different samples and the different reactions occurring within each sample. The results from RT-FTIR revealed that both esterification and epoxide ring-opening reactions occurred at 150 °C and 170 °C for all samples. The analysis further revealed that the rate of esterification was higher than the epoxy ring opening reaction although both occurred. A decrease in the profiles was seen at approximately 1000 s for the EMO-LOH reactions at 170 °C. This sudden decrease was due to evaporation of the sample. All samples analyzed at 130 °C showed that only an esterification occurred at this temperature. An increase in functionality (i.e. an increase in epoxides) resulted in a decrease in esterification rate.

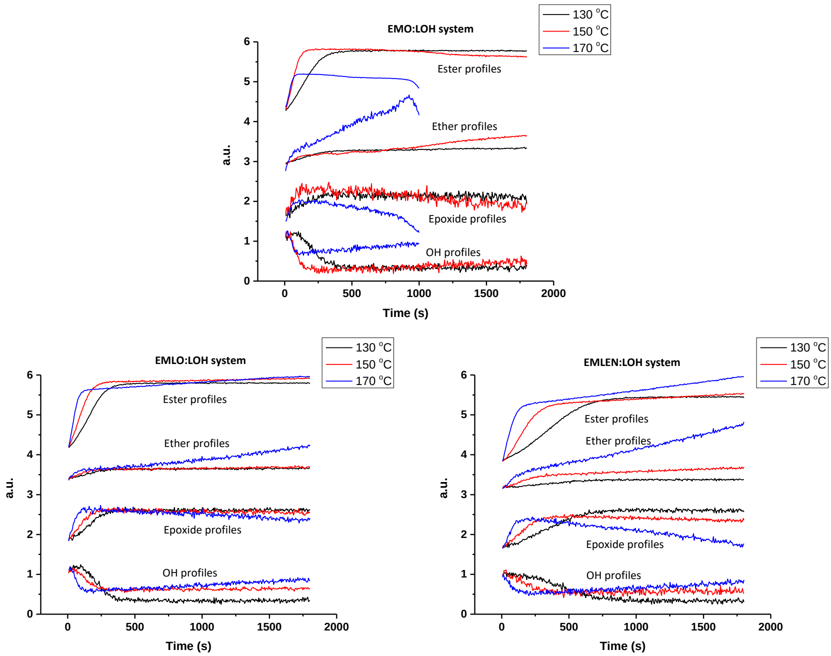

Figure 26: RT-FTIR of the reactions setup in Table 11 to investigate possible reaction pathways of e-FAME coil-coating formulation.

Table 12: Coil-coating sample formulations and the respective properties obtained. Viscosity (η) measurements were made on the actual formulation. T_g and contact angle were obtained from the cured coatings from respective formulation.

	Resin formulation		Thermoset	
Sample [a]	**e-FAME (wt%)**	**η (Pa s)** [d]	**T_g(°C)** [e]	**Contact angle (°)**
PE/Melamine [b]	0	3.5	32	88
FAME10 [c]	0	1.9	28	89
e-FAME5	5	2.1	26	90
e-FAME10	10	1.4	15	93
e-FAME15	15	0.9	-1	99
e-FAME20	20	0.7	0	99

Sample [f]	**e-FAME (wt%)**	**η (Pa s)**	**T_g(°C)**[d]	**Contact angle (°)**
FAME10 coil-coat	0	N/A	26	N/A
e-FAME5 coil-coat	5	N/A	26	N/A
e-FAME10 coil-coat	10	N/A	20	N/A

[a] Samples cured in lab oven at 170 °C, [b] Formulation without FAME or e-FAME. PE refers to polyester, [c] FAME10 represents formulation of polyester/melamine with 10wt% FAME, [d] Measured at 30 °C, [e] Characterized from DSC and was taken from the second heating, [f] Samples cured at PTE Coatings AB to simulate industrial coil-coating process at 330 °C giving peak metal temperature (PMT) 220-240 °C.

As a coil-coating formulation (Figure 24) we used a polyester-melamine resin system with increasing amount of e-FAME and added 4-dodecylbenzenesulfonic acid (DDBSA) as a catalyst. The different samples can be seen in Table 12.

Curing performance of the coil-coating formulations containing e-FAME (5-20 wt%) was evaluated. Samples for FTIR analysis were taken before and after intended curing. The resin formulation was spread on glass and steel substrate using an applicator producing a uniform film. The substrates were then placed in a preheated oven at 130 °C and 170 °C and were left for 30 min. Samples at 130 °C did not cure fully after 30 min in the oven. The time for these coatings was increased to 60 min; however, no tack-free coatings were formed. For samples at 170 °C, tack-free and clear coatings were obtained. The reaction between polyester-melamine and e-FAME was confirmed by FTIR (Figure 27). A shift in the carbonyl region from 1730 cm^{-1} to 1720 cm^{-1} was observed indicating a transesterification. In addition, both hydroxyl groups from polyester and epoxides from e-FAME decreased while an increase in the linear ether region was noticed, corroborating with results from RT-FTIR. A piece from each sample cured at 170 °C was taken for DSC characterization. DSC revealed that an increasing amount of e-FAME in the coil-coating formulation resulted in a decrease in T_g (Figure 28). From the evaluation using a laboratory oven, the most promising results, in comparison to FAME10, were e-FAME5 and e-FAME10. These formulations were also evaluated in a simulated coil-coating curing process on steel substrates. The curing of such process occurred at a peak metal temperature of about 220-240 °C for 30 seconds.[111,113] Clear and tack-free coatings were obtained from these experiments. DSC characterization (Figure 28) on these samples showed similar results to laboratory cured coatings. The best results, in comparison to FAME10, were obtained from e-FAME5 formulations. In addition, the DSC results suggest that more e-FAME are incorporated when comparing e-FAME10 and FAME10. Both formulations contain 10wt% fatty acid derivative, however a lower T_g was obtained by e-FAME10 indicating that more reactive diluent was incorporated in the final coating.

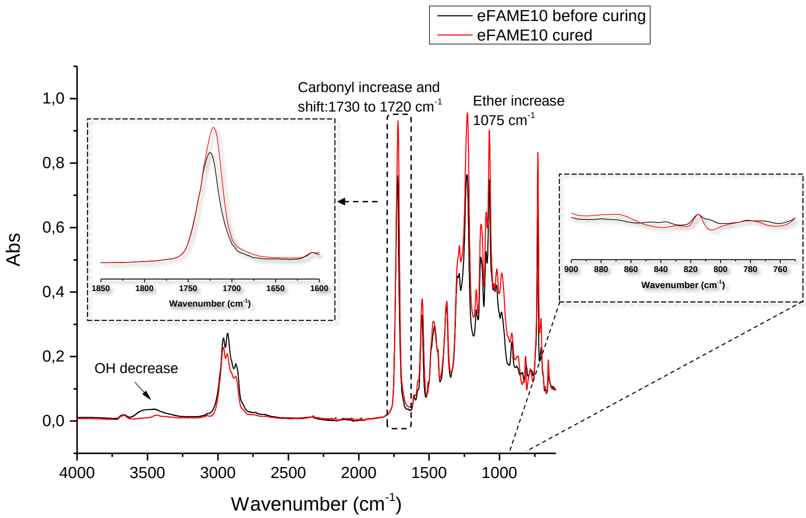

Figure 27: FTIR of e-FAME10 resin formulation and cured coating.

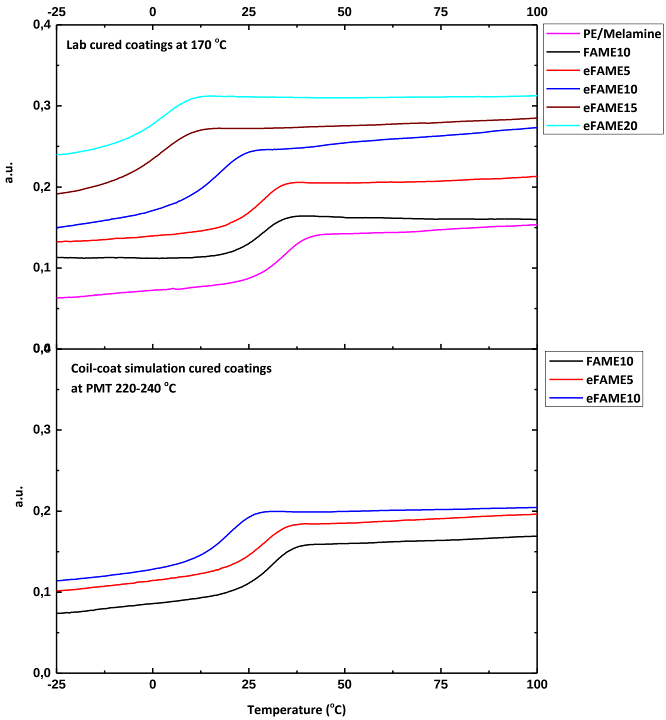

Figure 28: DSC thermograms from cured coatings. Above shows lab cured and below shows coil-coat simulated cured.

5. Conclusions

The overall theme of the thesis work was using epoxidized fatty acid derivatives, retrieved from renewable resources, in different coating applications. We have shown that it was possible to use renewable resources such as outer birch tree bark or epoxidized linseed oil to obtain epoxidized fatty acid derivatives. The retrieval process followed traditional chemistry used in industry. Outer birch tree bark was subjected to alkaline hydrolysis while epoxidized linseed oil to methanolysis in NaOH in order to obtain the epoxy fatty acid derivatives. Both procedures were harmless towards the epoxide functional group in our experimental settings; thus, the epoxy functionalities in the final extracted monomers were retained, as revealed by both NMR and FTIR.

Moreover, it was demonstrated that the lipase *Candida Antarctica* lipase-B (CALB) was a powerful and selective enzyme towards the formation of telechelic oligomers. We have shown that it was possible to use CALB as a tool in order to incorporate functional groups such as epoxides, alkenes and thiols into multifunctional resins. The synthetic procedure was mild and the products were formed from “one-pot” synthesis routes. In addition, we further demonstrated that the resins could form functional thermosets with the ability of surface post-modification. This was obtained from UV-curing the resins and a “left-over” functional group were available on the surface of the formed thermoset. The surface was modified with either a hydrophilic group (-OH) or hydrophobic group (-CF_3) resulting in surface contact angle change to 30° or 130° respectively.

An essential accomplishment of the thesis work was the demonstration of tailoring thermal and mechanical properties of bio-based epoxy thermosets. It was shown that retrieved epoxy fatty acid methyl esters, EMX, incorporated with the diglycidyl furan-2,5-dicarboxylate (DGFDC) were able to form high performance thermosets. This was demonstrated by changing the stoichiometry or number of functional group from EMX of the feed ratios resulting in tunable thermal and mechanical properties. Thermosets with T_g ranging from below 0 °C ranging to above 100 °C were obtained. In addition, EMX thermosets incorporated with bisphenol-A-diglycidyl ether were also made for comparison reason to the DGFDC.

An approach to show the ability of applying the e-FAME mixture to coil-coatings was made. Coil-coating of metal sheets is an industrially available procedure. Coil-coating resin formulations were made from e-FAME and compared with commercially used coil-coating formulations containing fatty acid methyl esters (FAME) obtained from rapeseed oil. The e-FAME mixture proved to be a reactive diluent similar to FAME. Increasing the amount of e-FAME in the formulation resulted in a lower viscosity of the formulation (i.e. an increased diluting effect as well as decreased thermal properties of the final cured coating). Moreover, cured coatings obtained from 5wt% e-FAME showed similar thermal properties to those obtained from 10wt% FAME. DSC results further revealed that e-FAME was more effective as a reactive diluent than FAME, indicated from lower T_g obtained when similar wt% were used.

Finally, a mistake in the lab led to a bio-based adhesive derived from outer birch tree bark. The fatty acid 9,10-epoxy-18-hydroxyoctadecanoid acid (EFA) proved to be a self-catalyzed monomer when heated resulting in adhesive properties. Model studies from compounds resembling EFA's structure demonstrated that both ring-opening and esterification reactions occur catalyzed by the presence of an acid. At elevated temperature above 100 °C the EFA cross-linked into an insoluble network with adhesive properties in a self-catalyzed process.

6. Future work

Regardless of the amount of work done for this thesis there is always room for further development and knowledge. Since the formed polymer materials were aimed for different coating applications further knowledge is needed from long-term properties and durability studies of the coatings. Moreover, the formed networks contained ester bonds which are prone to hydrolysis reactions; therefore, degradability studies should be considered as well. If the coatings degrade, what kind of adducts are formed, how they are formed and are they harmful or harmless to the environment?

In order for the retrieved epoxy fatty acid derivatives to compete with fossil based monomers the retrieval processes need to be scaled up and optimized. In addition, in order to utilize all components from the retrieval processes the by-products should be analyzed carefully. For instance, from the retrieval process of EFA from birch tree bark the soxhlet step resulted in a slightly yellowish product analyzed to be triterpenoid monomers such as betulin, lupeol and betulinic acid. The yield of the triterpenoids was 20% of the dry weight of the grinded outer birch tree bark. Furthermore, during the process of extracting EFA the different solutions along the way were subjected to centrifugation cycles. The "washing" steps probably extracted water soluble compounds. Moreover, the EFA was precipitated at pH 5.7 and then separated by centrifugation. The supernatant most likely contained other α,ω-fatty acid derivatives that are present in suberin structure. All of these different compounds might be interesting to investigate as raw material for chemical synthesis.

It was not possible to epoxidize DAFDC with CALB with our experimental setup. However, this approach should be further investigated in order to present a "greener" approach than using *m*-CPBA. A study on gradually adding catalytic amounts of hydrogen peroxide may provide more insights into the epoxidation. Another approach of introducing rigidity to the fatty acid derivatives may be obtained from lignin compounds as building-blocks instead of FDCA based. Both alternatives provide thermosets from renewable based monomers.

7. Acknowledgements

First and foremost I would like to acknowledge the Swedish research council, FORMAS (Grant No. 211-2013-70) for the financial support making the research possible for this thesis work.

Professor Mats Johansson, my main supervisor and mentor at the division of coating technology, your support during my research has been huge. In fact, you made it possible for me to pursue PhD studies. I cannot thank you enough for believing in me and accepting me as a PhD student. Nevertheless, I thank you for guiding me through all scientific hurdles I encountered during the research work. Your knowledge, wisdom and patience has been a great asset during my research.

I would like to thank my co-supervisor Mats Martinelle for all the scientific discussions in our BioPol meetings. Thank you for sharing your knowledge from the enzyme catalysis field.

To all my collaborators; Maja Finnveden, Stefan Semlitsch, Daniel Larsen, Tomas Deltin and Per-Erik Sundell. The projects would not have been possible without your commitment. Thank you for all the discussions and work during the experiments, analysis and manuscript preparations.

To all the members in Mats group and BioPol group thank you for making all meetings fun and sharing your knowledge.

Karin Odelius is very much thanked for taking the time to review and comment the work presented in the thesis.

I could not have imagined a better work place than the division of coating technology at KTH. I would first of all like to thank all the seniors: Anders Hult, Michael Malkoch, Eva Malmström, Linda Fogelström and Mats Johansson, for all of your time, effort and knowledge that you have put in our group. Further I want to express a huge acknowledgement all the members of the division, both old and new members, **the list is long**! It goes without saying - **THANK YOU ALL** for the support, work environment and all the scientific discussions.

A special acknowledgment goes to Joakim Engström and Marcus Jawerth for all the discussions and foremost for making a fun work environment at coating technology. I wish you all the best and success in your future endeavors.

Tahani and Tobias are thanked for the work regarding "PULS". I am glad that we could implement the "PULS" way of working at the division of coating technology.

Daniel Hutchinson is thanked for proof-reading the thesis and correcting all my has/have and was/were and commas and whatnots! ☺

Marcus Jawerth and Sara Brännström are very much thanked for their help with photoshop. That stuff is too advanced for me!

To all my friends outside KTH and family thank you for your support, motivation and interest in my studies and work.

My parents are thanked for motivating me to study and always pushing me to aim for the best. I thank you for all your support and that you always believe in me. You have provided the best environment for me to blossom. I hope that I have made you proud. My big brother, Nawres, is thanked for always being there when I needed you. Thank you for encouraging me through my whole life.

Last but not least, I want to express my biggest acknowledgement to the loves of my life, Emelie and Enzo. You are the reason for my happiness and joy in life. I cannot thank you enough for the support and love you have given me and I look forward to a future together with you.

8. References

1. The UN global goals. Available at: https://www.globalgoals.org/. (Accessed: 12th April 2019)

2. PlasticsEurope. Annual Review 2017-2018. *Assoc. Plast. Manuf.* (2018).

3. Geyer, R., Jambeck, J. & Law, K. Production, Use, And Fate Of All Plastics Ever Made. *Sci. Adv.* **3,** 25–29 (2017).

4. Maxwell, J. *Plastics in the Automotive Industry*. (Woodhead Publishing, 1994).

5. Piringer, O. G. & Baner, A. L. *Plastic packaging: interactions with food and pharmaceuticals*. (John Wiley & Sons, 2008).

6. Lyons, A. *Materials for Architects and Builders*. (Elsevier, 2007).

7. Philp, J. C., Bartsev, A., Ritchie, R. J., Baucher, M. A. & Guy, K. Bioplastics science from a policy vantage point. *N. Biotechnol.* **30,** 635–646 (2013).

8. Jambeck, J. R. *et al.* Plastic waste inputs from land into the ocean. *Science (80-.).* **347,** 768–771 (2015).

9. OPEC. OPEC: World Oil Outlook 2040. *Organ. Pet. Export. Ctries.* 1–214 (2017). doi:10.1190/1.1439163

10. Belgacem, M. N. & Gandini, A. *Monomers, Polymers and Composites from Renewable Resources*. *Elsevier* (Elsevier, 2008).

11. Bioplastics, E. Bioplastics Facts and Figures. (2018). doi:10.1136/bmj.1.5165.62

12. Mohanty, A. K., Misra, M. & Drzal, L. T. Sustainable Bio-Composites from Renewable Resources in Green Materials world. *J. Polym. Environ.* **10,** 19–26 (2002).

13. Budzianowski, W. M. High-value low-volume bioproducts coupled to bioenergies with potential to enhance business development of sustainable biorefineries. *Renew. Sustain. Energy Rev.* **70,** 793–804 (2017).

14. Kienle, R. H. & Ferguson, C. S. Alkyd resins as film-forming materials. *Ind. Eng. Chem.* **21,** 349–352 (1929).

15. Hofland, A. Alkyd resins: From down and out to alive and kicking. *Prog. Org. Coatings* **73,** 274–282 (2012).

16. Alexandr A. Berlin, Viktor F. Kablov, Andrey A. Pimerzin, S. S. Z. *Key Elements in Polymers for Engineers and Chemists From Data to Applications*. (Apple Academic Press, Inc, 2014).

17. Odian, G. *Prineples of polymerization 4the edition*. (John Wiley & Sons, IN, 2004). doi:10.1016/0168-3659(92)90108-4

18. Meier, M. A. R., Metzger, O. & Schubert, U. S. Plant oil renewable resources as green alternatives in polymer science. *Chem. Soc. Rev.* (2007). doi:10.1039/b703294c

19. Montero de Espinosa, L. & Meier, M. A. R. Plant oils: The perfect renewable resource for polymer science?! *Eur. Polym. J.* **47,** 837–852 (2011).

20. Xia, Y. & Larock, R. C. Vegetable oil-based polymeric materials: Synthesis, properties, and applications. *Green Chem.* **12,** 1893–1909 (2010).

21. Zhu, Y., Romain, C. & Williams, C. K. Sustainable polymers from renewable resources. *Nature* **540,** 354–362 (2016).

22. Stoye, D., Marwald, B. & Plehn, W. Paints and Coatings. *Ullmann's Encycl. Ind. Chem.* **25,** 1–28 (2012).

23. Kolattukudy, P. E. in *The Biochemistry of Plants* **4,** 571–645 (Academic Press, Inc, 1980).

24. Graça, J. Suberin: the biopolyester at the frontier of plants. *Polym. Chem.* **3,** 1–11 (2015).

25. Bernards, M. A. Demystifying suberin. *Can. J. Bot.* **80,** 227–240 (2002).

26. Graca, J. & Santos, S. Suberin: A Biopolyester of Plants' Skin. *Macromeluclar Biosci.* 128–135 (2007). doi:10.1002/mabi.200600218

27. Kolattukudy, P. E., Kronman, K. & Poulose, A. J. Determination of Structure and Composition of Suberin from the Roots of Carrot, Parsnip, Rutabaga, Turnip, Red Beet, and Sweet Potato by Combined Gas-Liquid Chromatography and Mass Spectrometry. *Plant Physiol.* **55,** 567–573 (1974).

28. Holloway, P. J. Some variations in the composition of suberin from the cork layers of higher plants. *Phytochemistry* **22,** 495–502 (1983).

29. Pereira, H. & Graca, J. Methanolysis of bark suberins: analysis of glycerol and acid monomers. *Phytochem. Anal.* **11,** 45–51 (2000).

30. Krasutsky, P. A. Birch bark research and development. *Nat. Prod. Rep.* **23,** 919–942 (2006).

31. Abyshev, A. Z., Agaev, É. M. & Guseinov, A. B. Studies of The Chemical Composition of Birch Bark Extracts (Cortex betula) From The Betulaceae Family. *Pharm. Chem. J.* **41,** 419–423 (2007).

32. Krasutsky, P. A., Carlson, R. M. & Nesterenko, V. V. Birch Bark Processing and The Isolation of Natural Products From Birch Bark. **1,** (2002).

33. Ekman, R. The Suberin Monomers and Triterpenoids from the Outer Bark of Betula verrucosa Ehrh. *Holzforschung* **37,** 205–211 (1983).

34. Pinto, P. C. R. O. *et al.* Quercus suber and Betula pendula outer barks as renewable sources of oleochemicals : A comparative study. *Ind. Crops Prod.* **9,** 126–132 (2008).

35. Backlund, B. & Nordström, M. Nya produkter från skogsråvara En översikt av läget 2014. *Innventia Rapp. nr. 577* (2014).

36. Gandini, A., Neto, C. P. & Silvestre, A. J. D. Suberin : A promising renewable resource for novel macromolecular materials. *Prog. Polym. Sci.* **31,** 878–892 (2006).

37. Naturvårdsverket. Available at: https://www.naturvardsverket.se/Documents/publikationer/620-8196-9.pdf. (Accessed: 10th April 2019)

38. Biermann, U. *et al.* New Syntheses with Oils and Fats as Renewable Raw Materials for the Chemical Industry. *Angew. Chemie* **39,** 2206–2224 (2000).

39. Lligadas, G., Ronda, J. C., Galià, M. & Cádiz, V. Renewable polymeric materials from vegetable oils: a perspective. *Mater. Today* **16,** 337–343 (2013).

40. United States Department of Agriculture. Global Oilseed Demand Growth Forecast to Outpace Production. (2017).

41. Gunstone, F. D., Harwood, J. L. & Dijkstra, A. J. *The Lipid Handbook*. (CRC press, 2007).

42. Eastman, W. *The History of the Linseed Oil Industry in the United States*. (T. S. Denison & Company, Inc., 1968).

43. Van De Mark, M. R. & Sandefur, K. Vegetable oils in paint and coatings. *Inf. - Int. News Fats, Oils Relat. Mater.* **16,** 478 (2005).

44. Erhan, S. Z. & Asadauskas, S. Lubricant basestocks from vegetable oils. *Ind. Crops Prod.* **11,** 277–282 (2000).

45. Derksen, J. T. P., Cuperus, F. P. & Kolster, P. Renewable resources in coatings technology : a review. *Prog. Org. Coatings* **27,** 45–53 (1996).

46. Mallégol, J., Gardette, J. L. & Lemaire, J. Long-term behavior of oil-based varnishes and paints. I. Spectroscopic analysis of curing drying oils. *JAOCS, J. Am. Oil Chem. Soc.* **76,** 967–976 (1999).

47. Wicks, Z. W. J., Jones, F. N., Pappas, P. S. & Wicks, D. A. *Organic Coatings Science and Technology*. (John Wiley & Sons, INC, 2007).

48. Lichtenthaler, F. W. & Peters, S. Carbohydrates as green raw materials for the chemical industry. *Comptes Rendus Chim.* **7,** 65–90 (2004).

49. Pan, X., Sengupta, P. & Webster, D. C. High biobased content epoxy-anhydride thermosets from epoxidized sucrose esters of fatty acids. *Biomacromolecules* **12,** 2416–2428 (2011).

50. Wool, R. P. *et al.* Development and application of triglyceride-based polymers and composites. *J. Appl. Polym. Sci.* **82,** 703–723 (2002).

51. Torron, S., Semlitsch, S., Martinelle, M. & Johansson, M. Biocatalytic Synthesis of Epoxy Resins from Fatty Acids as a Versatile Route for the Formation of Polymer Thermosets with Tunable Properties. *Biomacromolecules* **17,** 4003–4010 (2016).

52. Samuelsson, J. & Johansson, M. A study of fatty acid methyl esters with epoxy or alkyne functionalities. *JAOCS, J. Am. Oil Chem. Soc.* **78,** 1191–1196 (2001).

53. Sugihara, A. *et al.* Conversion of vegetable oil to biodiesel using immobilized Candida antarctica lipase. *J. Am. Oil Chem. Soc.* **76,** 789–793 (1999).

54. Meier, M. A. R., Metzger, J. O. & Schubert, U. S. Plant oil renewable resources as green alternatives in polymer science. *Chem. Soc. Rev.* **36,** 1788 (2007).

55. Perdue, R. E., Carlson, K. D. & Gilbert, M. G. Vernonia galamensis, Potential new crop source of epoxy acid. *Econ. Bot.* **40,** 54–68 (1986).

56. Baumann, H. *et al.* Natural Fats and Oils - Renewable Raw Materials for the Chemical Industry. *Angew. Chem. Int. Ed. Engl.* **27,** 41–62 (1988).

57. Björkling, F., Godtfredsen, S. E. & Kirk, O. Lipase-Mediated Formation of Peroxycarboxylic Acids Used in Catalytic Epoxidation of Alkenes. *J. Chem. Soc.* **22,** 1301–1303 (1990).

58. Björkling, F., Frykman, H., Godtfredsen, S. E. & Kirk, O. Lipase Catalyzed Synthesis of Peroxycarboxylic Acids andLipaseMediatedOxidations. *Tetrahedron* **48,** 4587–4592 (1992).

59. Warwel, S. & Rüsch gen. Klaas, M. Chemo-enzymatic epoxidation of unsaturated carboxylic acids. *J. Mol. Catal. B. Enzym.* **1,** 29–35 (1995).

60. Darensbourg, D. J. Making Plastics from Carbon Dioxide: Salen Metal Complexes as Catalysts for the Production of Polycarbonates from Epoxides and CO2. *Chem. Rev.* **107,** 2388–2410 (2007).

61. Hauenstein, O., Reiter, M., Agarwal, S., Rieger, B. & Greiner, A. Bio-based polycarbonate from limonene oxide and CO2 with high molecular weight, excellent thermal resistance, hardness and transparency. *Green Chem.* **18,** 760–770 (2016).

62. Ma, S. *et al.* Bio-based epoxy resin from itaconic acid and its thermosets cured with anhydride and comonomers. *Green Chem.* **15,** 245–254 (2013).

63. Vyazovkin, S. & Sbirrazzuoli, N. Mechanism and kinetics of epoxy-amine cure studied by differential scanning calorimetry. *Macromolecules* **29,** 1867–1873 (1996).

64. Palmese, G. R. & McCullough, R. L. Effect of epoxy–amine stoichiometry on cured resin material properties. *J. Appl. Polym. Sci.* **46,** 1863–1873 (1992).

65. Drauz, K., Gröker, H. & May, O. *Enzyme Catalysis in Organic Synthesis*. (WILEY-VCH Verlag, 2012).

66. Loos, K. *Biocatalysis in polymer chemistry*. (John Wiley & Sons, INC, 2011).

67. Silverman, R. B. *Organic Chemistry of Enzyme-Catalyzed Reactions*. (Academic press, 2002).

68. Behr, J.-P. *The Lock-and-Key Principle*. (John Wiley & Sons).

69. Kobayashi, S. *et al.* Enzymatic Polymerization. *Chem. Rev.* **101,** 3793–3818 (2001).

70. Anastas, P. & Eghbali, N. Green chemistry: Principles and practice. *Chem. Soc. Rev.* **39,** 301–312 (2010).

71. Scheirs, J. & Long, T. E. *Modern polyesters: chemistry and technology of polyesters and copolyesters*. (John Wiley & Sons, 2005).

72. Sandler, S. *Polymer syntheses*. **1,** (Academic Press, Inc, 1974).

73. Carrot, G., Hilborn, J., Hedrick, J. L. & Trollsås, M. Novel initiators for atom transfer radical and ring-opening polymerization: a new general method for the preparation of thiol-functional polymers. *Macromolecules* **32,** 5171–5173 (1999).

74. Liras, M., Quijada-Garrido, I., Palacios-Cuesta, M., Muñoz-Durieux, S. & García, O. Acetyl protected thiol methacrylic polymers as effective ligands to keep quantum dots in luminescent standby mode. *Polym. Chem.* **5,** 433–442 (2014).

75. Southan, A. *et al.* Side chain thiol-functionalized poly(ethylene glycol) by post-polymerization modification of hydroxyl groups: Synthesis, crosslinking and inkjet printing. *Polym. Chem.* **5,** 5350–5359 (2014).

76. Kobayashi, S. & Makino, A. Enzymatic Polymer Synthesis: An Opportunity for Green Polymer Chemistry. *Chem. Rev.* **109,** 5288–5353 (2009).

77. Okumura, S., Iwai, M. & Tominaga, Y. Synthesis of ester oligomer by aspergillus niger lipase. *Agric. Biol. Chem.* **48,** 2805–2808 (1984).

78. Anderson, E. M., Larsson, K. M. & Kirk, O. One biocatalyst - many applications: The use of Candida antarctica B-lipase in organic synthesis. *Biocatal. Biotransformation* **16,** 181–204 (1998).

79. Uyama, H. & Kobayashi, S. Enzyme-catalyzed polymerization to

functional polymers. *J. Mol. Catal. B Enzym.* **20,** 117–127 (2002).

80. Varma, I. K., Albertsson, A. C., Rajkhowa, R. & Srivastava, R. K. Enzyme catalyzed synthesis of polyesters. *Prog. Polym. Sci.* **30,** 949–981 (2005).

81. Uppenberg Jonas, Morgens, H., Shamkant, P. & Alwyn, J. T. The sequence, crystal structure determination and refinement of two crystal forms of lipase B from Candida antarctica. *Structure* **2,** 293–308 (1994).

82. Martinelle, M. *et al.* in *Handbook of Telechelic Polyesters, Polycarbonates, and Polyethers* 29–64 (Pan Stanford, 2017).

83. Hedfors, C., Hult, K. & Martinelle, M. Lipase chemoselectivity towards alcohol and thiol acyl acceptors in a transacylation reaction. *J. Mol. Catal. B Enzym.* **66,** 120–123 (2010).

84. Torron, S. & Johansson, M. Oxetane-terminated telechelic epoxy-functional polyesters as cationically polymerizable thermoset resins: Tuning the reactivity with structural design. *J. Polym. Sci. Part A Polym. Chem.* **53,** 2258–2266 (2015).

85. Eriksson, M. *et al.* One-pot enzymatic polycondensation to telechelic methacrylate-functional oligoesters used for film formation. *Polym. Chem.* **2,** 714–719 (2011).

86. Schönthaler, W. Thermosets. *Ullmann's Encycl. Ind. Chem.* **36,** 1–116 (2012).

87. Guo, Q. *Thermosets Structure, Properties and Applications*. (Elsevier, 2018).

88. Hoyle, C. E. & Bowman, C. N. Thiol-ene click chemistry. *Angew. Chemie - Int. Ed.* **49,** 1540–1573 (2010).

89. Sangermano, M. *et al.* Photopolymerization of epoxy coatings containing silica nanoparticles. *Prog. Org. Coatings* **54,** 134–138 (2005).

90. Ashcroft, W. R. *et al. Chemistry and Technology of Epoxy Resins*. (Springer Science & Business Media, 1993). doi:10.1007/978-94-011-2932-9

91. May, C. *Epoxy resins: chemistry and technology*. (Marcel Dekker,

Inc., 1988).

92. Decker, C. Photoinitiated Crosslinking Polymerisation. *Prog. Polym. Sci.* **21,** 593–650 (1996).

93. Hoyle, C. E., Lee, T. Y. & Roper, T. Thiol-enes: Chemistry of the past with promise for the future. *J. Polym. Sci. Part A Polym. Chem.* **42,** 5301–5338 (2004).

94. Sangermano, M. Advances in cationic photopolymerization. *Pure Appl. Chem.* **84,** 2089–2101 (2012).

95. Zhang, H., Massingill, J. L. & Woo, J. T. K. Low VOC, low viscosity UV cationic radiation-cured ink-jet ink system. *J. Coatings Technol.* **72,** 45–52 (2007).

96. Calvert, P. Inkjet printing for materials and devices. *Chem. Mater.* **13,** 3299–3305 (2001).

97. Decker, C., Moussa, K. & Bendaikha, T. Photodegradation of UV-Cured Coatings II. Polyeurethane-Acrylate Networks. *J. Polym. Sci. Part A Polym. Chem.* **29,** 739–747 (1991).

98. Chattopadhyay, D. K., Panda, S. S. & Raju, K. V. S. N. Thermal and mechanical properties of epoxy acrylate/methacrylates UV cured coatings. *Prog. Org. Coatings* **54,** 10–19 (2005).

99. Stansbury, J. W. Curing Dental Resins and Composites by Photopolymerization. *J. Esthet. Dent.* **12,** 300–308 (2000).

100. Carioscia, J. A., Lu, H., Stanbury, J. W. & Bowman, C. N. Thiol-ene oligomers as dental restorative materials. *Dent. Mater.* **21,** 1137–1143 (2005).

101. Granskog, V. Thiol-Ene/Yne Adhesives for Tissue Fixation. (KTH Royal Institute of Technology, 2018).

102. Crivello, J. V. & Lam, J. H. W. Diaryliodonium Salts. A New Class of Photoinitiators for Cationic Polymerization. *Macromolecules* **10,** 1307–1315 (1977).

103. Crivello, J. V. in *Initiators—poly-reactions—optical activity* 1–48 (Springer, 1984).

104. Decker, C., Nguyen Thi Viet, T. & Pham Thi, H. Photoinitiated cationic polymerization of epoxides. *Polym. Int.* **50,** 986–997 (2001).

105. Crivello, J. V. & Lee, J. L. Alkoxy-substituted diaryliodonium salt cationic photoinitiators. *J. Polym. Sci. Part A Polym. Chem.* **27,** 3951–3968 (1989).

106. Chiou, B.-S. & Khan, S. A. Real-Time FTIR and in Situ Rheological Studies on the UV Curing Kinetics of Thiol-ene Polymers. *Macromolecules* **30,** 7322–7328 (2002).

107. Cramer, N. B., Scott, J. P. & Bowman, C. N. Photopolymerizations of thiol-ene polymers without photoinitiators. *Macromolecules* **35,** 5361–5365 (2002).

108. O'Brien, A. K., Cramer, N. B. & Bowman, C. N. Oxygen inhibition in thiol-acrylate photopolymerizations. *J. Polym. Sci. Part A Polym. Chem.* **44,** 2007–2014 (2006).

109. Walling, C. & Helmreich, W. Reactivity and Reversibility in the Reaction of Thiyl Radicals with Olefins. *J. Am. Chem. Soc.* **81,** 1144–1148 (1959).

110. Jacobine, A. F. Thiol-ene photopolymers. *Radiat. Curing Polym. Sci. Technol.* **3,** 219–268 (1993).

111. Sander, J. *Coil Coating*. (Vincentz Network, 2014).

112. Johansson, K. Thermally Cured Coil-Coatings Utilizing Novel Resins and Fatty Acid Methyl Esters As Reactive Diluents. (Doctoral Thesis, 2008).

113. Goodwin, D. R. *Metal-coil surface-coating industry: background information for promulgated standards*. (Environmental Protection Agency, Research Triangle Park, NC (USA). Emission ..., 1982).

114. Lindeboom, J. Air-drying high solids alkyd pants for decorative coatings. *Prog. Org. Coatings* **34,** 147–151 (1997).

115. Johansson, K. & Johansson, M. Fatty acid methyl ester as reactive diluent in thermally cured solvent-borne coil-coatings-The effect of fatty acid pattern on the curing performance and final properties. *Prog. Org. Coatings* **63,** 155–159 (2008).

116. Larsen, D. B., Sønderbæk-Jørgensen, R., Duus, J. & Daugaard, A. E. Investigation of curing rates of bio-based thiol-ene films from diallyl 2,5- furandicaboxylate. *Eur. Polym. J.* **102,** 1–8 (2018).

117. Socrates, G. *Infrared and Raman characteristic group frequencies: tables and charts*. (John Wiley & Sons, 2004).

118. Statistiska Centralbyrån. Available at: https://www.scb.se/hitta-statistik/statistik-efter-amne/miljo/markanvandning/markanvandningen-i-sverige/pong/statistiknyhet/markanvandningen-i-sverige-20102/. (Accessed: 11th April 2019)

119. Skogsindustrierna. Available at: https://www.skogsindustrierna.se/skogsindustrin/branschstatistik/skogsindustrin-i-varlden/. (Accessed: 11th April 2019)

120. Zhu, W. *et al.* Metal and light free 'click' hydrogels for prevention of post-operative peritoneal adhesions. *Polym. Chem.* **5**, 2018–2026 (2014).

121. Kryuchkov, M. A. *et al.* Challenging activated monomer ring-opening polymerization for direct synthesis of thiol end-functionalized polyesters. *React. Funct. Polym.* **90**, 1–6 (2015).

122. Torron, S., Semlitsch, S., Martinelle, M. & Johansson, M. Polymer thermosets from multifunctional polyester resins based on renewable monomers. *Macromol. Chem. Phys.* **215**, 2198–2206 (2014).

123. Ajima, A. *et al.* Polymerization of 10-hydroxydecanoic acid in benzene with polyethylene glycol-modified lipase. *Biotechnol. Lett.* **7**, 303–306 (1985).

124. T. Werpy. & G. Petersen. Top Value Added Chemicals from Biomass Volume I — Results of Screening for Potential Candidates from Sugars and Synthesis Gas. **1**, (2004).

125. Production & Application of FDCA. Available at: https://www.avantium.com/yxy/products-applications/. (Accessed: 28th March 2019)

126. Prileschajew, N. Oxydation ungesättigter Verbindungen mittels organischer Superoxyde. *Berichte der Dtsch. Chem. Gesellschaft* **42**, 4811–4815 (1909).

127. Plesniar, B. in *OXIDATION IN ORGANIC CHEMISTRY* **5**, 211–294 (ACADEMIC PRESS, INC., 2012).

128. Kim, C., Traylor, T. G. & Perrin, C. L. MCPBA epoxidation of alkenes:

Reinvestigation of correlation between rate and ionization potential. *J. Am. Chem. Soc.* **120,** 9513–9516 (1998).

129. Dreyfuss, P. & Kennedy, J. P. Epoxidation with m-Chloroperbenzoic Acid: An Analytical Method for Determining Unsaturation of Olefins and Polymers. *Anal. Chem.* **47,** 771–774 (1975).

130. Sundell, P.-E. Cationic polymerization of vinyl ethers using iodonium and sulfonium salts. (Royal Institute of Technology, 1990).